Elemental Analysis of Glass by SEM-EDS, μXRF, LIBS and LA-ICP-MS

Award No: 2005-IJ-CX-K069

FINAL TECHNICAL REPORT

Jose Almirall, Ben Naes, Erica Cahoon and Tatiana Trejos

Department of Chemistry and Biochemistry and International Forensic Research Institute

Florida International University

Contact:

Jose Almirall, Professor and Director
Department of Chemistry and Biochemistry and
International Forensic Research Institute
Florida International University
11200 SW 8th Street, OE116
Miami, FL 33199
(305) 348-3917 *tel*
(305) 348-4485 *fax*
almirall@fiu.edu

Abstract

The transfer of small quantities of materials has become an important yet underutilized type of evidence at many crime scenes including hit-and-run accidents and other violent crimes. Although the utility of trace elemental analyses and comparisons for glass and paint fragments by sophisticated methods such as laser ablation inductively coupled plasma (LA-ICP-MS) has been shown to offer a high degree of discrimination between different sources of these materials, the high expense and sophistication of this technique has limited the adoption of this technology by the typical forensic laboratory, although there are now approximately 5 forensic laboratories in the U.S. with LA-ICP-MS capabilities. This 4.5 year research effort included an original award in 2005 and a continuation award in 2009 and has expanded on the PIs previous research in elemental analysis of materials (DoD/TSWG, end date 12/2002 and NIJ, end date 7/2005) to conduct a thorough evaluation of a number of elemental analysis methods (SEM-EDS, uXRF, LIBS and LA-ICP-MS) and compare the discrimination power between the methods used in most forensic laboratories for glass analysis. The continuation of the original proposal evaluated the analytical parameters for the LIBS analysis with an aim to create a more “standard” method that can be used by the operational forensic laboratory. The continuation award further advanced the selection of a “match criteria” based on LIBS (and uXRF) results for use in routine casework situations. This work was proposed as many operational laboratories in the US are adopting an elemental analysis component for glass and other trace evidence and to assist these labs in the decision-making process. Following the results from the original proposal project (end date 9/08), whereby one publication (see attached) concludes that the 266 nm excitation wavelength produces better precision and accuracy than 1064 nm or even 532 nm and a second publication compares the analytical merits and discrimination power of LA-ICP-MS, uXRF and LIBS, we then proposed to establish a standard method for glass analysis using LIBS. The first part of this project (2005-2008) developed a method for the forensic analysis of glass using LIBS including a collaboration with the Winefordner group at the University of

Florida and two publications resulted from this collaborative effort for a total of 8 publications from the work (See Appendix A for a list and a copy of all the publications derived from this work). Laser induced breakdown spectroscopy (LIBS) was shown to provide excellent discrimination potential for a glass set consisting of 41 automotive fragments recovered from 14 different vehicles. The discrimination power of LIBS was compared to two of the leading elemental analysis techniques, uXRF and LA-ICP-MS, and the results were similar; all methods generated >99% discrimination and the pairs found indistinguishable were correlated across the analytical methods. Included in this research was an extensive data analysis approach developed by our group to minimize Type II (false inclusion) and eliminate Type I (false exclusions) errors for LIBS spectral comparisons resulting in the recommendation of 10 ratios to be used for glass discrimination by LIBS. Therefore, it was concluded that LIBS, with its rapid analyses, lower cost, and reduced complexity, can provide a viable alternative to uXRF and LA-ICP-MS in forensic laboratories.

The second part of this grant (2008-2010) has resulted in the optimization of the LIBS method for glass examination and the dissemination of this information through scientific presentations at national and international meetings and during teaching workshops where forensic scientists participated as students. A total of 45 presentation were derived from this work (See Appendix B for a list of all the scientific presentations related to this grant).

Table of Contents

Executive Summary

This project addressed for a need in the continued development and validation of elemental analysis methods for the characterization of trace evidence for forensic purposes. Our group has endeavored to improve the value of trace evidence examinations, including the application of mature analytical techniques such as laser ablation inductively coupled plasma mass spectrometry (LA-ICP-MS), for the materials glass and paint over the last nine years and including the creation of a database of elemental data for over 700 different glass samples that illustrates the significance of a trace elemental "match". Forensic examiners can use this information to assist in the interpretation of comparisons of materials (known vs questioned) using trace elemental composition in order to provide to the court an opinion that is not ***overstated*** or ***understated***. The authors have also used LA-ICP-MS in actual cases and a Frye hearing has been successfully completed in Miami, Florida in 2004 for use in a hit-and-run accident fatality case. While LA-ICP-MS has been accepted as a powerful technique to discriminate between different glass samples through the comparison of the elemental data generated, it is an expensive and sophisticated technique that is out of the reach of many forensic laboratories. While the 2004 CTS Glass Analysis Summary of proficiency test results reported that 61% of the 122 respondents (74 laboratories) used elemental analysis as part of their analytical scheme, the vast majority of these laboratories employed scanning electron microscopy-energy dispersive spectrometry (SEM-EDS) as the method of elemental analysis comparisons. The recently published SWGMAT guidelines for elemental analysis of glass describe the limitations of sample size and shape and detection limits of SEM-EDS and our work (and the work of other workers)

also indicates that SEM-EDS should only be used either for classification between glass types or for the exclusion of an association when the glass samples have an obvious compositional difference. This is due to the extremely limited utility of SEM-EDS in differentiating between different glass samples as a result of the poor sensitivity (LOD of ~ 1000 ppm) and the fact that SEM-EDS is a qualitative analysis method that suffers from differences in analytical results depending on sample morphology (flat vs irregular surface). One aim of this work was to quantitatively determine the informing power of SEM-EDS as a comparison tool in glass analysis. These results have served to aid those laboratories using SEM-EDS in forming the opinion of the value of the additional information provided by SEM-EDS analysis and to limit opinions as to "significance of a match" when a "match" is fiund using this method. A number of forensic laboratories use micro X-Ray fluorescence spectrometry (uXRF) for comparing between glass samples as the detection limits of this method are improved an order of magnitude better than SEM-EDS and published reports do indicate good discrimination between different glass samples by uXRF. This technique, however, also suffers, from limitations of sample size (the technique is best used on samples measuring greater than 1 mm X 1mm) and sample shape (flat surfaces produce the best precision). The technique is also expensive and time consuming. The work reported here has quantitatively evaluated the method of uXRF in comparison to LA-ICP-MS and to compare these widely used methods to the emerging method of Laser Induced Breakdown Spectroscopy (LIBS) for the analysis of glass.

A second main purpose of this work was to thoroughly evaluate the LIBS technique for the analysis of glass in terms of performance. The analytical scheme for the use of LIBS was developed, validated and used for the analysis of a large number of glass samples.

Since the forensic application of LIBS was used as a comparison tool for materials, we also evaluated four different commercial LIBS systems manufactured by different companies (Ocean Optics using the Ocean Optics Spectrometer, Photon Machines using the Avantes Spectrometer, Applied Spectra, and Foster and Freeman). In addition, we used a laboratory built system using an Andor Mechelle spectrometer coupled to an Andor ICCD camera in an effort to first evaluate the detector performance and then to recommend a "standard" method that produces high quality data. Analytical parameters for the four LIBS commercial instruments were optimized for the acquisition of LIBS spectra from the analysis of glass. Equally important, this project developed a comprehensive data analysis strategy for the comparison of LIBS spectra. Finally, the discrimination power of LIBS was compared to the discrimination power of SEM-EDS, XRF, and LA-ICP-MS for the same set of glass samples.

Glass was chosen as an initial matrix of interest due to our extensive experience with the material, the availability of matrix-matched standards for calibration and the forensic interest of glass as trace evidence. The same elemental analysis methods can later be applied to other matrices of forensic interest. As a result of our interactions with several instrument companies, there are several commercial bench-top LIBS instruments that can be used in a forensic laboratory and more manufacturers are now making commercial instruments available in the $ $ 60. k - $ 70. k price range. This work has thoroughly evaluate the commercial LIBS instruments for their forensic utility and provided feedback to the manufacturers to improve the instrumentation for use in forensic applications.

Although the utility of trace elemental analyses and comparisons for glass and paint fragments by sophisticated methods such as laser ablation inductively coupled plasma

(LA-ICP-MS) has been shown to offer a high degree of discrimination between different sources of these materials, the high expense and sophistication of this technique has limited the adoption of this technology by the typical forensic laboratory, although there are now approximately 5 forensic laboratories in the U.S. with LA-ICP-MS capabilities. This 4.5 year research effort included an original award in 2005 and a continuation award in 2009 and has expanded on the PIs previous research in elemental analysis of materials (DoD/TSWG, end date 12/2002 and NIJ, end date 7/2005) to conduct a thorough evaluation of a number of elemental analysis methods (SEM-EDS, uXRF, LIBS and LA-ICP-MS) and compare the discrimination power between the methods used in most forensic laboratories for glass analysis. The continuation of the original proposal evaluated the analytical parameters for the LIBS analysis with an aim to create a more "standard" method that can be used by the operational forensic laboratory. The continuation award further advanced the selection of a "match criteria" based on LIBS (and uXRF) results for use in routine casework situations. This work was proposed as many operational laboratories in the US are adopting an elemental analysis component for glass and other trace evidence and to assist these labs in the decision-making process. Following the results from the original proposal project (end date 9/08), whereby one publication (see attached) concludes that the 266 nm excitation wavelength produces better precision and accuracy than 1064 nm or even 532 nm and a second publication compares the analytical merits and discrimination power of LA-ICP-MS, uXRF and LIBS, we then proposed to establish a standard method for glass analysis using LIBS. The first part of this project (2005-2008) developed a method for the forensic analysis of glass using LIBS including a collaboration with the Winefordner group at the University of Florida and two publications resulted from this collaborative effort for a total of 8 publications from the work (See Appendix A for a list and a copy of all the publications derived from this work). Laser induced breakdown spectroscopy (LIBS) was shown to provide excellent discrimination potential for a glass set consisting of 41 automotive fragments recovered from 14 different vehicles. The discrimination power of LIBS was compared to two of the leading elemental analysis techniques, uXRF and LA-ICP-MS, and the results were similar; all methods generated >99% discrimination and the pairs found indistinguishable were correlated across the analytical methods. Included in this

research was an extensive data analysis approach developed by our group to minimize Type II (false inclusion) and eliminate Type I (false exclusions) errors for LIBS spectral comparisons resulting in the recommendation of 10 ratios to be used for glass discrimination by LIBS. Therefore, it was concluded that LIBS, with its rapid analyses, lower cost, and reduced complexity, can provide a viable alternative to uXRF and LA-ICP-MS in forensic laboratories.

The work presented in this report has outlined results that will certainly help the forensic community with respect to glass analysis. In the first part of the research, a nanosecond LA-ICP-MS was proven to offer similar figures of merit for the forensic analysis of glass (in terms of accuracy, precision and discrimination power) when compared to femtosecond LA-ICP-MS, which was hypothetically expected to outperform nanosecond LA-ICP-MS. It was also shown that an internal standard was necessary in order to obtain accurate and precise results for both methods, meaning that internal and matrix matched standardization are important to ensure optimum quantitative analyses by LA-ICP-MS, whether the laser be a nanosecond source or a femtosecond source. The observed comparable results by nanosecond and femtosecond LA-ICP-MS is attributed to the utilization of quantification from a glass matrix-matched standard, which is readily available to the forensic scientific community. In cases where a matrix-matched standard is not available (and in some cases a good internal standard is not available), femtosecond LA-ICP-MS could provide improved results (in terms of precision and discrimination potential) over nanosecond LA-ICP-MS analyses for the same matrix.

Laser induced breakdown spectroscopy (LIBS) was introduced for the analysis of glass, which was shown to provide similar discrimination potential (>99% discrimination) for an automotive glass sample set of forensic interest when compared to two of the leading techniques in elemental analysis, uXRF and LA-ICP-MS. A strict protocol for data evaluation of LIBS spectra was evaluated and then followed to minimize Type I (false exclusion) errors and eliminate Type II (false inclusion) errors, which ultimately addresses the concerns outlined by the National Research Council's report on forensic analyses. Overall, a method using LIBS has been developed, optimized, and validated for the forensic analysis of float glass, which due to its low cost,

reduced complexity (user friendliness), faster analysis time, and capability of being a portable technique, makes LIBS a viable alternative to XRF and LA-ICP-MS for the elemental analysis of glass.

The second part of this grant (2008-2010) has resulted in the optimization of the LIBS method for glass examination and the dissemination of this information through scientific presentations at national and international meetings and during teaching workshops where forensic scientists participated as students. A total of 45 presentation were derived from this work (See Appendix B for a list of all the scientific presentations related to this grant).

Chapter 1.

1.1 *Statement of the Problem*

Analytical methods for the forensic analysis and comparison of glass by using the elemental composition are presented. A study that assesses and compares the figures of merit and performance of an existing technique, glass analysis by LA-ICP-MS, using two different laser systems is also presented. With respect to the forensic glass studies, it is important to establish first and foremost the necessity of elemental analysis for the characterization and discrimination of float glass. It has been established and concluded in previous studies that refractive index measurements do not often provide the discrimination power necessary for forensic glass comparisons **[1-2, 3, 5-7]**. Since manufacturers target similar refractive indices and thus only a small degree of variation between different source may be detected, the lack of discrimination power can ultimately lead to Type II errors (false inclusion), meaning that a pair was found indistinguishable when the fragments originated from different sources. Elemental analysis helps to minimize the potential to commit these errors and thus increases the discrimination capability.

In chapter 2 below, the advantages of femtosecond laser ablation (LA) ICP-MS, as described in the literature, will be assessed for the forensic analysis of glass and the resulting figures of merit will be compared to the less complex and less expensive approach of nanosecond LA-ICP-MS. Studies using different quantification approaches in addition to the use (or non-use) of an internal standard will be presented. The latter concept is particularly important to the scientific community because if femtosecond LA-ICP-MS can provide accurate and precise results without the need of an internal standard, then analyses on other matrices where an internal standard is not available could be readily performed (i.e. paint).

Finally, in chapters 3 and 4 below a method (including an extensive data analysis study) using laser induced breakdown spectroscopy (LIBS) will be presented and the results compared to two of the leading techniques in elemental analysis of materials, micro-XRF and LA-ICP-MS. The significance of this study is that LIBS is expected to provide a viable alternative to the aforementioned approaches with respect to

discrimination power (all other techniques generated 99%+ discrimination potential). LIBS provides faster analysis times, a reduction in complexity of use, and the instrumentation can be purchased at a fraction of the cost as compared to micro-XRF and LA-ICP-MS.

1.2 Literature Citations and Review

The literature is cited throughout this report as necessary and a review of the relevant literature is included in the following chapters.

1.3 Rationale for the Research

This research was initiated due to the lack of available information regarding elemental analysis of glass and other materials using LIBS. It was expected at the initiation of this research that LIBS, would indeed, provide excellent evidence of discrimination between different glass samples and association between galss samples originating from the same source.

Chapter 2.

2. ANALYTICAL COMPARISON OF NANOSECOND AND FEMTOSECOND LA-ICP-MS FOR THE ELEMENTAL ANALYSIS OF GLASS

2.1 Glass Matrix

By definition, glass is referred to any amorphous transparent or translucent material that is comprised of a mixture of silicates and was inherently produced by fusion and eventual solidification from the molten state (of these silicates) in the absence of crystallization. The main constituent in glass is silicate (or from an elemental viewpoint, silicon) and for commercial glass manufacturing the source most utilized to acquire the silicate backbone is sand (SiO_2). Typically, other oxides are added during the manufacturing of glass such as lime (CaO), soda ash (Na_2O), and potash (K_2O) which assist with reducing key (and economical) factors like the melting point of SiO_2 and

viscosity. Other raw materials (including recycled materials) are added for various reasons depending on the desired finished product such as lead oxide (PbO) to increase refractivity, boron oxide (B_2O_3) to lower thermal expansion [and create borosilicate glass], and aluminum oxide (Al_2O_3) to increase durability, as well as various coloring (or decolorizing) agents, oxidizing (or reducing) agents, etc [4].

Thus, there exists any number of possible elemental components (and combinations of elements) in glass, which are attributed either directly (or indirectly) to the raw materials or to the manufacturing process itself. Given this premise, there is a high degree of variation among the elemental profiles for glasses circulating in the population of glass by which characterization and forensic (elemental) analysis is possible.

Many types of glass exist in the general population, but one of (if not) the most common type encountered in forensic casework involves float glass which encompasses many sub-types under that classification (i.e. automotive windshields, side and rear windows and architectural glass). The term float comes from the process by which these flat glasses are produced wherein the molten fused glass floats on a bed of liquid tin en route to cooling; the process is favorable to manufacturers because the finished product doesn't require additional finishing methods (unless they are desired) and uniform thickness of the glass is achieved [4]. All of the presented research involves characterization and discrimination of float glass sources. The short list of crimes where glass evidence is often encountered includes: burglaries, vandalism, and hit-and-runs, to name a few.

2.2 Elemental Analysis of Glass

Several analytical methods exist for determining the elemental composition of glass, including inductively coupled plasma mass spectrometry (ICP-MS), X-ray fluorescence (XRF), scanning electron microscopy with energy dispersive X-ray spectroscopy (SEM-EDS), and laser ablation-inductively coupled plasma mass spectrometry (LA-ICP-MS), each of which has its advantages and disadvantages [5]. The comparison of the given techniques and others (i.e. atomic absorption, neutron activation, and ICP atomic emission spectroscopy) has been reviewed extensively in the literature

[6-7]. Two of those techniques (XRF and LA-ICP-MS) will be compared to the analysis of glass by LIBS in the next chapter, and additional details regarding background information for those techniques are presented there.

Of these techniques, LA-ICP-MS offers increased sensitivity, the capability to perform quantitative analysis over a wide range of elements and isotopes, and excellent precision, all of which translate into improved discrimination potential. Despite these advantages, the major disadvantage of this technique is the associated cost of the instrumentation, which has prevented many forensic laboratories from acquiring a LA-ICP-MS.

Previous research that helped with the advancement of the forensic analysis of glass using elemental analysis includes the work by Hickman in 1986 [1], who used ICP-AES to determine the concentrations of Mg, Ba, Mn, Fe, Al and Sr for a glass sample set/database of 1350 samples [1]. With these elemental concentrations, combined with refractive index measurements and multi-variant statistics (squared mean Euclidian distances), Hickman was able to classify casework glass samples into two groups, sheet and non-sheet glasses; and when tested, a high degree of accurate classification over a six year period was obtained [1]. Ryland targeted classification of glass samples into the two most common types of forensic glass evidence, container glass and sheet glass in 1986 [2]. The approach was to first compare Mg concentrations by SEM-microprobe analysis with the premise that sheet glass samples typically contain greater than 2% Mg while container glass samples typically contain less than .1% [2]; by this method, 81% of container glasses were correctly classified. A Ca/Fe ratio using XRF was then used to attempt further classification and it was found that 93% proper classification was achieved by this method [2]. Koons et al reported the use of ICP-AES in 1988 to determine the element composition of of 184 glass samples (concentrations of Al, Ba, Mg, Fe, Sr, Mn, Ca, Na, and Ti) to discriminate sheet glass from container glass [47]. Koons et al used principal component analysis (PCA) and cluster analysis to correctly classify 180 of the 184 samples [47]. Additionally, complete discrimination by manufacturing plant was obtained via cluster analysis [47] meaning that the elemental composition of glass samples can potentially be traced back to the glass manufacturer. Becker et al concluded in 2001 that the discrimination of float glass samples using

several elemental analysis techniques, including SEM-EDX, μ-XRF, and ICP-MS, was possible where refractive index measurements found such samples indistinguishable [48], Becker et al also pointed out that despite discriminating the sample set, the former two techniques (SEM-EDX and μ-XRF) were less discriminating than ICP-MS. The improved discrimination was a product of sensitivity where ICP-MS could detect (and quantify) distinguishing elements in the sample set where the other elemental analysis techniques could not [48].

Furthermore, a protocol was developed and later published by the American Society of Testing and Materials (ASTM) for the forensic analysis of glass by dissolution ICP-MS (ASTM E-2330-2004) [8]. This protocol, initially drafted in our research group, provided the details on how to digest and compare glass fragments for forensic purposes. The digestion method consists of the use of HNO_3, HF, and HCl in combination with the induction of heat to completely dissolve (solubilize) the glass in preparation for dissolution ICP-MS [8]. The next step in the evolution of glass analysis was to compare a relatively new technique at the time, laser ablation ICP-MS (LA-ICP-MS), to digestion ICP-MS in terms of the important analytical figures of merit such as accuracy, precision, and discrimination power. It was concluded that LA-ICP-MS provided similar figures of merit for glass samples of similar and differing sources of origin [9]. This was an important step for reasons specified in the laser ablation description section, which highlighted replacing the difficult and dangerous digestion methodology with a solid sampling technique that required almost no sample preparation. Given the fractionation issues encountered with nanosecond LA-ICP-MS, the fractionation concept was studied for the analysis of glass. From this research, it was demonstrated that fractionation was not a factor in the accurate quantitative analysis of glass by LA-ICP-MS [10]. Furthermore, sampling strategies for the forensic analysis of glass by LA-ICP-MS detailed the significance of representative sampling for container and headlamp glass; it was also concluded that float glass is homogeneous even at the mass range sampled by laser ablation, typically less than a microgram of material removed [11]. In addition, it was shown that accurate and comparable results (for standard reference materials NIST 612 and NIST 610) can be obtained for various sized fragments down to 0.1 mm in size using LA-ICP-MS [12]. Latkoczy et al, as part of a collaborative and inter-laboratory

effort reported good agreement in the same glass sample results performed in different laboratories. In addition, a new set of glass reference materials, FGS01 and FGS02, were introduced for the quantification of glass as an alternative to NIST 612 and 610. These standards were more similar in composition (or better matrix-matched) to actual float glass samples and analyses showed that the use of these glasses for quantification provided an improvement in accuracy [13].

The next step involving the forensic analysis of glass by our group and collaborators included the application of laser induced breakdown spectroscopy (LIBS), which will be discussed in the next chapter of this report, and whether or not the performance advantages of femtosecond laser ablation ICP-MS (fs-LA-ICP-MS) over nanosecond laser ablation ICP-MS (ns-LA-ICP-MS) reported in the literature equated into improved figures of merit (accuracy, precision, limits of detection, and discrimination) for the analysis of float glass. The ultimate question asked was whether the additional cost of a femtosecond laser could be justified for the continued advancement of glass analysis and other applications of forensic interest.

2.3 Methodology

2.3.1 Instrumentation

2.3.1.1 Introduction

One-half of the presented data was generated at FIU while the other half of the data was generated by the collaborator in this project, Dr. Jhanis Gonzalez, who works for Professor Richard Russo at the Lawrence Berkeley National Laboratory (LBNL) in Berkeley, CA. The aforementioned group was a key contributor to this project because they maintain a femtosecond laser ablation ICP-MS system which allowed for the comparison to our nanosecond laser ablation ICP-MS system. The Russo group is one of only a handful of groups performing analytical chemistry that utilize such instrumentation (femtosecond LA-ICP-MS) at the time the project was begun. Nonetheless, all of the respective data analyses for both the nanosecond and femtosecond LA-ICP-MS were performed at FIU.

2.3.1.2 Laser Ablation Principles and Considerations

Laser ablation is a solid sampling technique used to remove finite amounts of matter from a solid matrix via use of a laser. The ablation of the material from the surface occurs by combination of complex processes including melting, fusion, sublimation, vaporization and finally explosion (of the material from the matrix) [16]. The ablation process and the degree of mass removal is dependent on the sample's (or material's) ability to absorb energy from the laser pulse. Upon laser to sample interaction, if the energy of the laser pulse exceeds the binding energy of the atomic infrastructure of the material, an atom is ejected. With laser ablation, the amount of material removed (or ablated) from the material is inversely proportional to the duration of the pulse (or pulse width). Thus, nanosecond laser sources require laser intensities of 10^8-10^9 W/cm^2 [101-102].

The ablation process is characterized by either thermal or non-thermal mechanisms or both, which is dependent on the wavelength and the pulse width of the laser [16, 53-55]. With thermal mechanisms, sample melting and vaporization occur as a result of absorption of the laser light by the electrons in the sample lattice, this absorbed energy is then transferred into the sample lattice. As a result, fractionation could result via thermal mechanisms which are inherent on the differing phase transitions of the elements [51,52]. On the contrary, non-thermal mechanisms are characterized by the elimination of the discussed heating affects (encountered with the thermal processes). Moreover, when the energy of the photon exceeds the binding energy of the atoms, the laser radiation can rupture the sample (atomic) lattice without heat dissipation into the sample, which results in an explosive ejection of atoms and ions that directly represent the sample composition (no observed fractionation) [53-55].

During the ablation process, four thresholds occur at different time intervals, as presented in Figure 1 [16]. On the femtosecond time scale, the absorption of the laser pulse (or energy) causes electronic excitation. Electrons are subsequently emitted from the sample surface on the picosecond time scale. When additional laser energy is pulsed into the sample lattice, vaporization and ionization occur via collisions with the surrounding gas causing a laser induced plasma (or plume) to be generated on the nanosecond time scale [16]. This laser induced plasma (or emission of light) is the basis for the LIBS experiment. During this stage of the ablation process, plasma shielding can occur where the laser beam interacts with the growing plasma causing the laser energy to

be absorbed or reflected by the generated plasma [16]. Plasma shielding can be avoided by using shorter laser wavelengths in which the laser beam more efficiently penetrates into the plasma ultimately causing more efficient bond breaking and less fractionation. Finally, on the microsecond time scale, the particles are ejected from the surface by means of normal evaporation and explosive boiling [16].

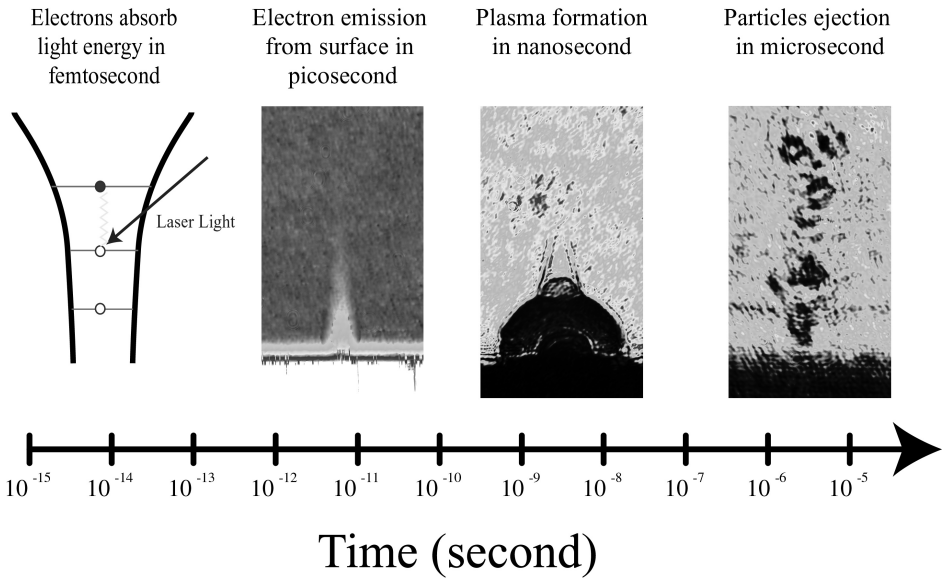

Figure 1. Time scale and events associated with laser ablation. Figure was extracted from Russo RE, Mao X, Mao SS (2002) Anal Chem 74:70A-77A [16]

A typical laser system contains a laser source (typically, a nanosecond Nd:YAG source operating at 1064nm or one of its harmonic wavelengths, 532nm, 266nm, 213nm, etc.), fairly simple optics (a series of mirrors and lens needed for focusing the laser beam), a camera (for viewing the sample surface), a pressurized ablation cell (which has a carrier gas line running into and out of the cell), and a computer to control the collective system (where ablation parameters are controlled and changed) [14-15]. The carrier gas line coming out of the ablation chamber is then directly attached to the inductively coupled plasma (ICP) source, which atomizes and ionizes the ablated mass en route to detection via mass analysis (MS) or emission spectroscopy (OES or AES) [14-15].

2.3.1.2.1 Advantages of Laser Ablation

In comparison to traditional dissolution techniques, LA offers many advantages without compromising selectivity and sensitivity. Dissolution methods involve sampling

a portion of the solid material under investigation, placing the sample aliquot (usually milligrams) into a digestion vessel, adding concentrated acid(s) and finally digesting the material with use of a controlled heating device over a specified period of time (usually several hours or more). The sample digests are then diluted into a specified volume and ultimately analyzed. Such methodology is prone to contamination issues, including contributions from the sample container, from the added solvents (acids and water), and from the atmosphere. Digestion methods are also prone to sample loss or even analyte loss (volatile components) and depending on the method applied there are often serious exposure-related hazards that must be considered when heating concentrated acid solutions [14-15].

Laser ablation, however, requires virtually no sample preparation, which eliminates many of the problems associated with dissolution methods and increases sample throughput [14]. Another major advantage for laser ablation offers over its dissolution counterpart is related to sample size requirements which are generally in the sub-microgram range for most ablation methods versus milligrams of material (or more) needed for dissolution methods [14]. Reduced sample sizes are especially beneficial to certain applications (i.e. forensics) where there are often limited amounts of sample. As a result to the small amount of sample consumed, laser ablation is considered a nondestructive technique (or virtually nondestructive) and hence classified as a microchemical analysis [16].

2.3.1.2.2 Disadvantages of Laser Ablation

As with any analytical technique or instrument, there are several disadvantages that are important to consider and ultimately decipher if the advantages outweigh the disadvantages. Since laser ablation is a direct sampling technique some issues are unavoidable. First of all, since the consumption of sample is much less in comparison to dissolution methodologies (see the smaller sample size requirements stated in the previous paragraph), the sample is (or can be) less representative of the bulk (whereas dissolution/digestion procedures are considered bulk analyses). Nonetheless, multiple sampling locations can increase sample representation and thus enhance characterization. In addition, the smaller amount of mass entering the ICP-MS for laser ablation typically

translates into higher detection limits. In terms of quantitative analysis, quantification of the ablated mass is often difficult where matrix matched standard reference materials are not available. The reason matrix match standards are important is because accurate quantification by laser ablation (ICP-MS) is directly correlated to the ablation rate (the amount of mass ablated per laser pulse), which is inherent to the respective sample matrix [14]. Thus, if the sample set under investigation is of different composition than the standard being used for quantitative analysis, the laser to sample interaction (and ultimately sampling) is different and which makes the association inaccurate. In other words, even with similar compositions some assumptions must be made when performing quantitative analysis by LA-ICP-MS. However, despite the lack of matrix-matched standards, some applications have utilized the NIST series glass standards for quantification and successful results have been obtained in terms of accuracy nevertheless this protocol is not recommended [14]. Another disadvantage and probably the most studied variable related to laser ablation is elemental fractionation, which occurs (or is defined as when) the ablated mass is different in composition from the bulk sample [14]. Fractionation can be intrinsic (matrix related) and/or it can occur as a function of the ablation process (dependency on laser irradiance, wavelength, pulse width, and pulse duration); fractionation can even be a product of ablation transport (in relation to carrier gas and the ablation chamber/tubing) and/or it can occur within the inductively coupled plasma itself [14]. Research has shown that utilizing a higher laser irradiance and shorter pulse durations significantly reduces fractionation, these variables aid in producing smaller particle size distributions that are more readily transported and efficiently atomized/ionized in the inductively coupled plasma [14].

2.3.1.2.3 Femtosecond Laser Ablation Principles

All of the work referenced previously involved the use of nanosecond laser ablation systems. It has been reported extensively in the literature that nanosecond laser ablation is associated with elemental fractionation which can occur in any stage of the ablation process, including upon laser-sample (laser-matter) interaction, during sample transport into the inductively coupled plasma (ICP), which is partially dependent on particle size distributions, and during particle vaporization inside the ICP itself, which is

characterized by plasma conditions and particle size distributions. The degree of fractionation in each of these stages not only is dependent on the laser pulse duration (or pulse length) but on other parameters related to the laser utilized (i.e. wavelength, energy, repetition rate, etc) as well as the physical-chemical properties related to the sample matrix itself (i.e. absorptivity, thermal diffusion, composition, etc). Nonetheless, laser wavelength and pulse duration are believed to be two primary parameters influencing laser ablation and fractionation effects. In the case of glass samples, the ablation efficiency (ablated mass per pulse), particle size, and particle size distributions are dependent on wavelength [17-19].

Nevertheless, the influence and effects of laser wavelength is more evident when low photon energy (IR) wavelengths are compared to high photon energy (UV) wavelengths and such effects are negligible when a UV laser (i.e. 213nm) is compared to another UV laser (i.e. 266nm) if the laser energies are similar. Several studies have shown that improved ablation efficiency, smaller particle size, and narrower particle distributions were obtained when shifting from IR to UV wavelength lasers [17-19]. The other factor that must be considered which can improve the ablation characteristics (efficiency, particle size distributions) is laser pulse duration or often called simply the pulse length of the laser. It has been well documented that when laser energy is delivered on the nanosecond time scale (pulse length), the transfer time is sufficient to thermally dissipate the photon energy (from the applied laser) into the sample lattice as heat which in turn causes sample melting and elemental fractionation [14, 20-21]. However, with femtosecond laser ablation, due to its shorter pulse duration most of the photon energy from the laser pulse is converted into kinetic energy and thereby use of femtosecond laser sources minimizes the thermal affects and fractionation associated with nanosecond laser ablation [14, 20-21]. This thermal related (and sample melting) phenomenon can be visually seen in Figure 2, which shows interferometry images (analysis performed by Jhanis Gonzalez as part of this study) for both femtosecond and nanosecond laser ablation operated at the same parameters (line scan, the same spot size and the same fluence was used for both laser systems). As you can see, there is a clear the difference in the heating effects of nanosecond laser pulses (thermal dissipation of the laser energy into

the sample matrix) which ultimately causes the melting issue (observed on the sides of the ablated line) mentioned previously.

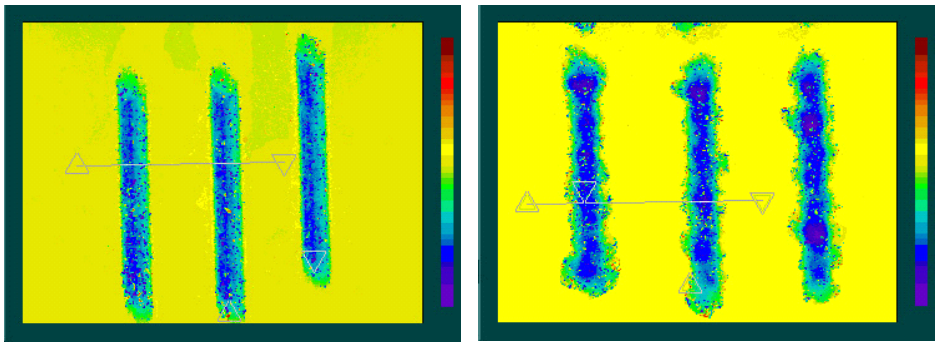

(a) fs-LA-ICP-MS, NIST 612 (b) ns-LA-ICP-MS, NIST 612

Figure 2. Interferometry images depicting thermal dissipation effects (and subsequent melting) of NIST 612 using nanosecond LA-ICP-MS, (a) represents femtosecond and (b) represents nanosecond laser ablation, respectively. Images courtesy of Jhanis Gonzalez at the Lawrence Berkeley National Laboratory (LBNL).

Russo et al concluded that femtosecond LA-ICP-MS was superior to nanosecond LA-ICP-MS with respect to accuracy and precision for the analysis of brass and NIST silicate glasses [20]. Poitrasson et al found similar results with his comparison of the two laser systems, namely for the analysis of monzanite, zircon, and NIST glasses [23]. Gonzalez et al found that femtosecond laser ablation improved the internal (the precision within a single ablation spot) and external repeatability (the precision between ablation spots) of the ICP-MS measurements of NIST 610 and NIST 612 glasses [24]. Gonzalez et al in a separate study ultimately concluded that the use of femtosecond laser ablation improved the accuracy and precision over nanosecond laser ablation for the analysis of lead in zinc-based alloy standard reference materials without use of an internal standard [24]. In addition, Poitrasson et al concluded that femtosecond LA-ICP-MS was less matrix dependent in comparison to nanosecond LA-ICP-MS [23], which is consequently the overall consensus within the laser ablation community.

The question in this study was whether or not the performance advantages of femtosecond laser ablation ICP-MS (fs-LA-ICP-MS) over nanosecond laser ablation ICP-MS (ns-LA-ICP-MS) reported in the literature equates into improved figures of merit (accuracy, precision, limits of detection, and discrimination) for the analysis of

float glass standards and actual casework samples. And, ultimately, if the additional cost of a femtosecond laser could be justified for continued advancement of glass analysis and other applications of forensic interest.

2.3.1.3 Laser Ablation Systems Description

2.3.1.3.1 Nanosecond Laser Ablation

The first of two laser ablation systems utilized in this study was the one housed in the Almirall laboratory, which is a New Wave Research UP213 system (Fremont, CA), which is a Nd:YAG, Q-switched laser operating at 213nm and a pulse width of 4ns. Besides the laser, the laser ablation system is equipped with a number of key components that make the ablation and then mass transfer into the ICP-MS possible. The optics are important for directing the laser pulses on the targeted area of a sample, the sample is housed in an ablation cell that has a constant gas flow of helium going into and out of the cell (and into the inductively coupled plasma). The provided software allows for ablation parameters to be altered according to the sample matrix, including energy, spot size, repetition rate, ablation mode, etc. The exact parameters for this particular system are reported in Table 1 which can be found after the next section.

2.3.1.3.2 Femtosecond Laser Ablation

The second laser ablation system utilized in this study is located in the Lawrence Berkeley National Laboratory in Berkeley, CA. This particular laser ablation system is essentially a home-made system. The laser itself, as listed in Table 1, is a Spectra Physics Hybrid (Waltham, MA) system operating at 266nm and a pulse width of 150fs. The delivery and sample viewing optics were the same as with the nanosecond laser ablation system described previously. In their case, the laser has been stripped from a New Wave Research UP213 system (Fremont, CA), at any rate the sole functioning of this device (ablation cell, gas flows, delivery optics, etc.) are exactly the same as the device in the Almirall laboratory. The laser is directed from an optics table by a series of mirrors and lenses and into the stationary laser ablation system where sample selection and analysis is performed.

Table 1. Femtosecond and nanosecond LA-ICP-MS parameters used in this study.

	Femtosecond LA-ICP-MS (LBNL)	Nanosecond LA-ICP-MS (FIU)
Laser Ablation	**Spectra Physics Hybrid (150 fs)**	**New Wave Research Nd:YAG (4 ns)**
Wavelength	266 nm	213 nm
Energy	0.2 mJ	0.6 mJ
Repetition Rate	10 Hz	10 Hz
Spot Size	45 µm	55 µm
Fluence	13 J/cm^2	25 J/cm^2
ICP-MS	**VG-Elemental PQ3**	**Perkin Elmer Elan DRC II**
RF Power	1400 W	1500 W
Plasma Gas Flow (Ar)	14.2 L/min	16.0 L/min
Auxillary Gas Flow (Ar)	1.0 L/min	1.0 L/min
Carrier Gas Flow (He)	0.9 L/min	0.9 L/min
Make-up Gas Flow (Ar)	0.9 L/min	0.9 L/min
Detector	Standard Mode	Standard Mode
Dwell Time	8.0 ms	8.3 ms

2.3.1.4 ICP-MS Principles and Considerations

Inductively coupled plasma techniques, namely ICP-AES and ICP-MS, have revolutionized elemental and isotopic composition determinations for a variety of matrices, including solid, liquid, and gases; furthermore, the advantage of such techniques is that they offer rapid, simultaneous, multi-element determinations for elements at major, minor, and trace concentrations [25].

The basic construction of a typical ICP-MS instrument can be broken down into five distinct parts: (1) a sample introduction system, (2) the inductively coupled plasma, (3) an interface between the plasma and the spectrometer regions, (4) a set of ion focusing lenses, and (5) the mass spectrometer, all of which have serve separate and important functions but work collectively together to achieve the desired analytical result. Traditionally, samples are introduced into the inductively coupled plasma (ICP) as an aerosol, which is produced from a aqueous sample and use of a pneumatic nebulizer (equipped with a spray chamber). Nevertheless, other states of matter can also be introduced into the ICP, one of which is covered and utilized extensively in the work presented in this report, laser ablation. This solid sampling technique which introduces sub-micrograms of solid material into the ICP will be discussed in detail in a later section.

These small particles of matter (solid, liquid, or gaseous) generated by the sample introduction system are introduced into the argon inductively coupled plasma by a steady stream of argon (or in the case of the laser ablation experiments presented here use a mixture of argon and helium). The inductively coupled plasma is generated and sustained with a combination of several mechanisms. The plasma is initially generated via a spark from a Tesla coil, which introduces seed (or free) electrons into the torch which is characterized as an argon-rich atmosphere (provided by a constant flow of argon). This steady flow of argon contained within a quartz tube (or torch) is located in the center of a copper induction (or load) coil through which a high frequency electric current is continuously passed (the applied current is produced by a radio frequency generator). An intense magnetic field is generated by a combination of the applied electric current and continual collisions between neutral argon atoms and free electrons. The abundance of ionic species and electrons result and thus sustain (or maintain) the inductively coupled plasma even during sample introduction. Hence, the argon plasma offers great stability and robustness in a chemically inert environment. On a technical level, the self-sustaining argon ICP generates high gas temperatures (~4500-8000K), high electron temperatures (~8000-10000K) and high electron densities (~10^{15} cm^{-3}). With such plasma characteristics and a high ionization potential (15.75 eV), the inductively coupled plasma is capable of vaporizing, atomizing, exciting, and ionizing most elements on the periodic table [25].

The newly formed ions generated by the ICP are then extracted by a series of interface cones (sample and skimmer cones) which take the ions from the atmospheric conditions needed by the plasma and into the high vacuum conditions necessary for mass spectrometry. Before the ions reach the mass spectrometer, they pass through a set of ion lenses which help direct or focus the ions into the mass analyzer. Though several types exist, the most common type of mass analyzer found in ICP-MS systems is the quadrupole, which is consequently the type of analyzer used to generate the research presented in this report. The quadrupole uses a combination of direct (+) and a radio frequency alternating currents (-) to separate the ions based on their respective mass to charge ratios. By applying different voltages to the four cylindrical rods of the quadrupole system, specific masses are selectively removed while others are allowed to

pass through and ultimately reach the detector. The typical resolving power for most commercial quadrupole instruments is 300, which is equivalent to one mass unit [25]. The detector converts the generated signal into a mass spectrum where the magnitude of a given peak is proportional to concentration of that species in the measured sample. A schematic of a typical ICP-MS system can be found in Figure 3.

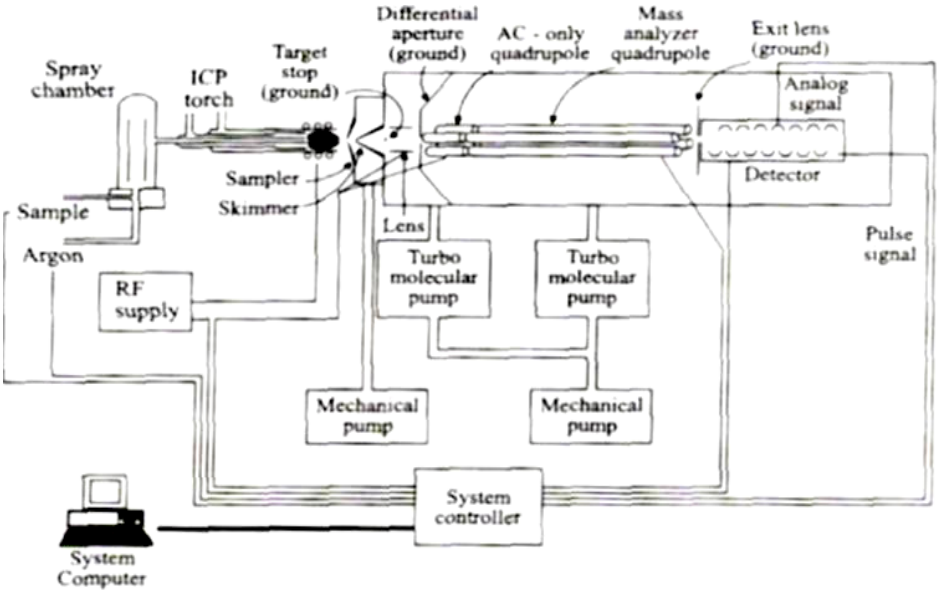

Figure 3. Schematic of a typical ICP-MS system [26].

2.3.1.4.1 ICP-MS Interferences

The main sources of spectral interferences encountered in ICP-MS are as follows: (1) isobaric interferences, which is direct overlap of an isotope of one element which has the same nominal mass as an isotope of another, (2) doubly-charge species which are the result of an atom losing two electrons in the inductively coupled plasma, and (3) polyatomic ions, which are the combination of two or more atomic species and are the main source of interfering species encountered in inductively coupled plasma mass spectrometry [25]. Polyatomic species typically arise (and thus show up on a mass spectrum) from the sample preparation steps, the atmosphere, or from the sample matrix itself. Oxygen, nitrogen, hydrogen to name a few, and high concentration of sodium and calcium, when recombined with other atomic species cause spectra overlap for certain isotopes, which often cannot be separated using a typical quadrupole mass analyzer. Instead use of quadrupole instruments equipped dynamic reaction cells or magnetic

sector detectors are needed for correct detection of certain isotopes, such as $^{56}Fe^{+}$ which is not resolved from $^{40}Ar^{16}O^{+}$ by quadrupole ICP-MS. The two options listed here are very different mechanisms by which say ^{56}Fe can be correctly identified and quantified. With the utilization of a dynamic reaction cell, a reactant gas is added (i.e. CH_4) (into a cell inserted prior to the quadrupole mass analyzer) and reacts with the interfering species to form a new polyatomic ion and thus the parent ion can then be detected [26-30]. With magnetic sector instruments the resolving power can be up to R=10000 in high resolution mode, which in turn allows for the separation of species that are 0.01 mass units apart, like $^{56}Fe^{+}$ from $^{40}Ar^{16}O^{+}$, as versus 1 mass unit separation for quadrupole detectors. In brief, for magnetic sector detectors, the ion beam is doubly focused. The ions are first accelerated through the ion lenses and into a magnetic field, which is dispersive with respect to the mass to charge ratio, then the ions reach the electrostatic analyzer which separates ions with respect to energy [31]. Nevertheless, although both types of instruments were available for use at FIU, they were not used for the projects summarized in this work.

2.3.1.5 ICP-MS Systems Descriptions

Each of the two ICP-MS systems used in this study was a quadrupole based system, which consequently is the most typical ICP-MS utilized in forensic laboratories. The ICP-MS used at FIU was a Perkin Elmer 6100 DRC II instrument (Waltham, MA) while the LBNL instrument was a VG-Elemental PQ3 ICP-MS (Waltham, MA), both of which were used and maintained under optimized conditions following the criteria stated in the next paragraph/section.

2.3.1.6 LA-ICP-MS Optimization

Collectively, the two systems (laser ablation plus ICP-MS) described above were optimized using NIST 612 (National Institute of Standards, Boulder, CO) as the reference standard, which has elemental concentrations for various elements in the at ~40ppm. The optimization protocol involves ablating the said reference glass at 100% energy, a spot size of 55µm, and use of the line (or rastering) ablation mode (10µm/sec scan rate); the gas flows into and out of the ablation cell, as well as the make-up gas going into the ICP,

were adjusted to achieve the desired ICP-MS values per element described below. The optimization criteria followed for both instrumental setups consisted of the following isotopes and their respective targeted values (in parentheses): ^{7}Li (>1500cps), ^{49}Ti (>1000cps), ^{57}Fe (>800cps), ^{59}Co (>8000cps), ^{139}La (>10000cps), ^{140}Ce (>14000cps), ^{232}Th (>3000cps), ^{238}U (>3000cps), background signal at 220 mass units (<2cps), fractionation (Th/U=1±0.2), % doubly charged species (Ca^{++}<3%), and % oxides (ThO<3%). The latter three criteria are important to reduce the degree of sample fractionation as well as to reduce polyatomic interferences, which is especially important for glass matrices where a large percentage of oxides present. The observed values were recorded on a daily basis for quality control purposes and for preventive (or regular) maintenance-related issues.

2.3.2 Sample Descriptions and Preparation

2.3.2.1 Glass Source Descriptions

2.3.2.1.1 Glass Standards

\ One glass standard reference material, NIST 612, and two reference glasses, FGS01 and FGS02 (BKA, Germany), were utilized as the external calibration source(s) for all data presented in this section of the report. The first of which is a certified standard reference material that has concentrations at ~40ppm for each element in the matrix while the latter two calibration sources (FGS01 and FGS02) are matrix matched glasses produced to resemble typical elemental compositions found in actual float glass samples meaning that the concentrations vary by element as versus a consistent concentration across all elements found with NIST 612 [13]. In this work, the availability of these reference glasses and NIST 612 were used to quantify float glass standard reference material NIST 1831, as well as a float glass sample set of forensic interest which will be described in the next section. The concentrations per element utilized for quantification purposes (or reference purposes in the case of NIST 1831) in this study can be found in Table 2. In the associated table, the stated concentrations stem from previous work, the superscript “a” represents values reported by NIST [8], the superscript “b” from Latkoczy’s paper [13], and “c” from Trahey’s work [32].

Table 2. Reference concentrations (in ppm) utilized for quantification and evaluation purposes.

element	NIST 612[a]	FGS01[b]	FGS02[b]	NIST 1831[c]
Mg	77.44	23900	23400	21166
Al	11164.6	1500	7400	6381
Ti	48.11	69	326	114
Rb	31.63	8.6	35	6.11
Sr	76.15	57	253	89.11
Zr	35.99	49	223	43.35
Ba	37.74	40	199	31.51
La	35.77	4.3	18	2.12
Ce	38.35	5.2	23	4.53
Nd	35.24	5.1	25	1.69
Hf	34.77	3.2	15	1.09

2.3.2.1.2 Casework Glass Sample Set

The glass set used in this study includes 11 forensic casework float glass samples provided by the Florida Department of Law Enforcement (FDLE, Orlando, FL). The given sample set includes both architectural and automotive glass fragments, which were found to be indistinguishable by refractive index measurements (each of the associated samples had a refractive index of 1.5186). Such details were provided by Scott Ryland at FDLE. Nonetheless, this particular case (or set of glass samples) demonstrates the importance of why elemental analysis is often necessary to compliment refractive index measurements and thus ensure accurate discrimination of glass samples collected at crime scenes. If refractive index measurements were the sole discrimination technique used, there would be 0% discrimination and a high degree of Type II errors (false inclustion). The sample descriptions for the FDLE casework glass set can be found in Table 3.

Table 3. Glass source descriptions for the casework sample set provided by FDLE. Thickness measurements ±0.1mm.

source ID	thickness (mm)	glass type	source description
W103	4.81	float	vehicle side window
W107	4.93	float	vehicle side window
W129	4.87	non-float	sliding glass door
W132	5.61	float	display case
W152	5.82	float	bathroom window (outer pane)
W153	4.75	non-float	bathroom window patterned (inner pane)
W165	4.73	float	store window
W174	4.89	float	vehicle side window
W206	5.69	float	store window
W232	5.63	float	business window

2.3.2.2 Sample Preparation

Each of the standards and samples mentioned above were treated as independent samples and thus same the general format of sample preparation was followed for each. Although bulk sample preparation steps are not necessary for LA-ICP-MS analyses due its solid sampling approach, each sample fragment in this study was initially rinsed with 5% HNO_3 prior to analysis to remove surface contaminants. Sample analysis was performed on the non-float side.

2.3.3 Experimental

2.3.3.1 Element Menu

The element/isotope menu for this study represented 11 elements, with the majority representing minor and trace elements/isotopes that are typically utilized for forensic glass comparisons [91-94,1-3,9]. More specifically, the isotopes analyzed in this study included: ^{25}Mg, ^{27}Al, ^{49}Ti, ^{85}Rb, ^{88}Sr, ^{90}Zr, ^{137}Ba, ^{139}La, ^{140}Ce, ^{146}Nd and ^{178}Hf. The internal standard used in this study is ^{29}Si because silicon the most abundant element found in float glass and due to its large concentration (>70%) and the associated signal, the concentration difference between glass samples is considered to be negligible.

2.3.3.1 Sample Analysis

Three different quantification strategies were employed and each standard (NIST 612, FGS01 and FGS02) was thus treated as a single source calibrator and run at the

beginning and end of the respective analytical sequences. A minimum of three replicates of each calibration standard were run and the average intensity of the standard replicates was then used to quantify the float glass standard (NIST 1831) and actual casework glass samples. Nine replicates of NIST 1831 were analyzed for each LA-ICP-MS system; three replicates of NIST 1831 were run at the beginning of the analytical sequence, three were run in the middle, and three replicates were run at the end to provide a comprehensive assessment across the entire analytical sequence and to study the variation across the entire run. Between the sample replicates/analyses of NIST 1831, three replicates of each casework glass sample (W103, W107, etc) were analyzed.

2.3.4 Data Analysis

2.3.4.1 Data Integration and Quantification

Integration of each time-resolved spectra, associated to a given sample replicate and generated by the ICP-MS, was conducted using Glitter software (Macquarie, Australia), where the count rate (or intensity) per isotope was determined via the difference between the raw analytical signal (ablation) and the gas blank signal (pre-ablation). Once the respective count rate per isotope was found, further data analysis was carried out utilizing Microsoft Excel (Redmond, WA) and the quantification equation found below [33] along with the stated reference values for each standard listed in Table 2. In Equation 1, "S" represents normalized sensitivity, "RAN" represents the count rate for the sample ("SAM"), "RIS" is the count rate for the internal standard, and finally "CAN" represents concentration of the sample and calibration standard respectively [33].

$$C_{AN_{SAM}} = \frac{R_{AN_{SAM}}}{S} \qquad where \qquad S = \frac{R_{AN_{CAL}}}{C_{AN_{CAL}}} \frac{R_{IS_{SAM}}}{R_{IS_{CAL}}} \frac{C_{IS_{CAL}}}{C_{IS_{SAM}}} \tag{1}$$

The quantification approach described by Longerich et al [17] was utilized to quantify (see the previous equation) float glass standard reference material NIST 1831 and the casework glass samples. It should be noted that for quantification purposes, and in relation to the provided equation, the concentration of silicon (used as the internal standard) was assumed to be the same for all glass samples analyzed; therefore, the right hand side of the equation (C_{IS}/C_{IS}) would equal 1 which simplifies the equation. Each

(single point) quantification approach (NIST 612, FGS01, and FGS02, respectively) was applied to each sample replicate utilizing the same analytical signal, with and without the use of the internal standard ^{29}Si. In addition, the exact same glass fragments and standards were analyzed in each lab utilizing the associated setups outlined in Table 1.

2.3.4.2 Accuracy and Precision

Comparisons of accuracy (in terms of % bias) and precision (% RSD) were evaluated for the analysis of NIST 1831 as was the precision across the casework sample set. For this study accuracy was expressed in terms of % bias, which is the percent error of each individual mean when compared to the respective reference value. Negative percent bias values indicate concentration values that were below the stated reference values and positive % bias values indicate values that were found to be greater than the said reference values.

2.3.4.3 Method Detection Limits

Method detection limits were determined by using Equation 2, which represents Poisson counting statistics at the 99% confidence interval. In the given equation, *B* represents the total number of counts in the background interval (data integration of the blank segment of each time-resolved spectra just prior to the onset of ablation). The detection limit per element provided in Table 8 (found in the results and discussion section) are actually the calculated average method detection limit for all the respective samples in the sequence.

$$MDL = 4.65\sqrt{4B} \qquad (2)$$

2.3.4.4 Discrimination

Discrimination analysis for the 11 casework glass sample set was performed using Systat 11 (Chicago, IL) wherein the concentrations, found via the quantification strategies discussed above, in the respective glass samples were compared utilizing analysis of variance (ANOVA) function with Tukey's honestly significance test (HSD) at the 95% confidence interval. Using the N(N-1)/2 rule, for 11 samples the total number of possible (pairwise) comparisons was 55. For the pairs found indistinguishable by ANOVA, a t-test at the 95% confidence interval was used to further discriminate the associated samples. After application of the t-test, if the two statistical approaches did not

discriminate the samples, then the samples were hence indistinguishable meaning that they were from the same source of origin. More specifically, these glass samples probably originated from the same manufacturing plant and were produced at about the same time.

2.4 Results and Discussion

2.4.1 Accuracy and Precision

2.4.1.1 Nanosecond LA-ICP-MS

For nanosecond (ns) LA-ICP-MS, shown in Table 4, considering all of the elements collectively, the accuracy of NIST 1831 was improved (decreased bias) with use of the calibration standard FGS02. The use of NIST 612 as a calibration standard produced the least accuracy, as predicted and shown in a previous study [13]. The associated bias using FGS02 as the calibration standard was found to be less than 5% for most elements. In the case of Sr and Zr, though more different than the reference value (especially in the case of Zr with a bias of 21.2%), the values are in good agreement with the cumulative (mean) values for NIST 1831 obtained in this laboratory over a four year time period (~100 replicates), namely 76.3ppm and 31.2ppm, respectively. Excellent precision for the nine replicates was obtained (<5%) for the majority of the elements, as shown in Figure 4. The only exceptions are Nd and Hf, where the concentrations are approaching the limits of detection which thus explains why higher %RSDs were obtained. Since the same analytical signal (via integration of the time-resolved spectra) was utilized for each quantification approach, therefore the precision was the same regardless of the quantification approach used.

Table 4. Quantification results for NIST 1831 using different calibration standards, nanosecond LA-ICP-MS, with use of an internal standard.

	NIST 612			FGS01			FGS02		
element	mean	std.dev.	% bias	mean	std.dev.	% bias	mean	std.dev.	% bias
Mg	26248.41	293.22	24.0	20656.69	230.76	-2.4	21276.69	237.68	0.5
Al	6512.83	111.95	2.1	5978.86	102.78	-6.3	6367.88	109.46	-0.2
Ti	134.57	5.67	18.3	106.94	4.51	-6.0	110.53	4.66	-2.9
Rb	6.03	0.25	-1.3	6.96	0.29	14.0	5.80	0.24	-5.1
Sr	78.58	2.44	-11.8	79.85	2.48	-10.4	78.77	2.44	-11.6
Zr	32.01	1.30	-26.2	34.14	1.39	-21.2	34.15	1.39	-21.2
Ba	30.38	1.65	-3.6	29.84	1.62	-5.3	31.58	1.72	0.2
La	2.24	0.11	5.5	2.27	0.11	7.2	2.23	0.11	5.4
Ce	4.53	0.26	0.1	4.74	0.28	4.7	4.49	0.26	-0.8
Nd	1.84	0.24	8.9	1.74	0.22	2.9	1.77	0.23	4.8
Hf	0.84	0.11	-22.6	0.94	0.13	-13.6	0.96	0.13	-12.3

Comparing Table 4 (quantification with use of an internal standard) and Table 5 (quantification without an internal standard), particularly looking at the quantification with FGS02 (the best calibration approach for nanosecond LA-ICP-MS), better results are observed when an internal standard is used. Additionally, a systematic difference between the two data sets (~10%) is also observed, which then improves the accuracy for given elements (i.e. Sr and Zr).

Table 5. Quantification results for NIST 1831 using different calibration standards, nanosecond LA-ICP-MS, with*out* use of an internal standard.

	NIST 612			FGS01			FGS02		
element	mean	std.dev.	% bias	mean	std.dev.	% bias	mean	std.dev.	% bias
Mg	26317.11	3429.53	24.3	25181.78	3281.58	19.0	23838.05	3106.47	12.6
Al	6521.09	769.24	2.2	7278.08	858.53	14.1	7123.78	840.33	11.6
Ti	134.66	15.66	18.3	130.19	15.14	14.4	123.56	14.37	8.6
Rb	6.03	0.70	-1.3	8.48	0.99	38.8	6.49	0.75	6.1
Sr	78.79	10.69	-11.6	97.41	13.22	9.3	88.31	11.98	-0.9
Zr	32.05	4.06	-26.1	41.58	5.27	-4.1	38.24	4.85	-11.8
Ba	30.52	4.99	-3.2	36.52	5.98	15.9	35.51	5.81	12.7
La	2.24	0.32	5.8	2.77	0.40	30.8	2.51	0.36	18.2
Ce	4.54	0.63	0.3	5.77	0.81	27.5	5.04	0.70	11.2
Nd	1.85	0.42	9.7	2.14	0.48	26.5	2.00	0.45	18.1
Hf	0.85	0.19	-22.0	1.15	0.26	5.6	1.08	0.24	-1.1

This improvement in accuracy is not only correlated with the observed systematic difference but is also correlated to an increase in imprecision where the precision is 2 - 4 times better when the internal standard is used for quantification (as noted in Figure 4). Since precision is more critical than bias when comparing/discriminating glass samples analyzed at the same time, quantification with an internal standard is recommended.

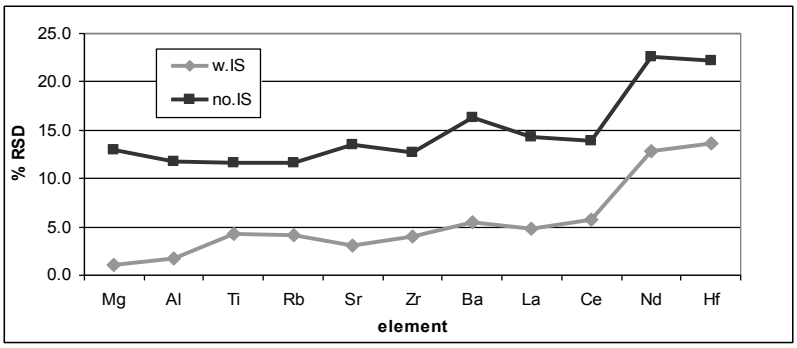

Figure 4. Precision results for NIST 1831 for nanosecond LA-ICP-MS, with vs. with*out* use of an internal standard.

2.4.1.2 Femtosecond LA-ICP-MS

With femtosecond (fs) LA-ICP-MS (see Tables 6 and 7) the accuracy of NIST 1831 was also improved by approximately 2-4% when utilizing an internal standard (FGS01). The tables also suggest a ~ 2X improvement in the precision for quantification with an internal standard over a given analytical sequence, which ultimately affects discrimination potential.

Table 6. Quantification results for NIST 1831 using different calibration standards, femtosecond LA-ICP-MS, with use of an internal standard.

	NIST 612			FGS01			FGS02		
element	mean	std.dev.	% bias	mean	std.dev.	% bias	mean	std.dev.	% bias
Mg	22647.30	357.18	7.0	19776.78	311.91	-6.6	19576.78	308.76	-7.5
Al	5209.76	40.32	-18.4	5163.93	39.97	-19.1	5451.55	42.19	-14.6
Ti	126.07	5.19	10.8	110.42	4.55	-3.0	106.56	4.39	-6.4
Rb	6.51	0.38	6.6	7.75	0.46	26.9	5.90	0.35	-3.4
Sr	83.05	4.39	-6.8	88.25	4.67	-1.0	83.71	4.43	-6.1
Zr	30.68	1.67	-29.2	34.72	1.89	-19.9	32.18	1.75	-25.8
Ba	29.55	1.73	-6.2	30.79	1.80	-2.3	29.98	1.75	-4.9
La	2.02	0.11	-4.8	2.21	0.12	4.3	1.96	0.11	-7.7
Ce	4.57	0.27	0.9	4.95	0.29	9.3	4.26	0.25	-5.9
Nd	1.65	0.10	-2.2	1.75	0.10	3.3	1.64	0.10	-2.8
Hf	0.83	0.09	-23.8	0.99	0.11	-9.2	0.93	0.10	-14.2

As observed, there is no significant difference in accuracy between the two instrumental setups (see Tables 4 and 6). For quantification with NIST 612, better accuracy was obtained for 3 out of the 11 elements (Al, Rb, and Ba) with ns-LA-ICP-MS while Mg, Ti, Sr, and Nd faired better for femtosecond LA-ICP-MS. Nonetheless, this is likely just a product of the ICP-MS (utilized) wherein certain elements may perform better on one instrument versus another. For the other two quantification approaches,

FGS01 provided greater overall accuracy for femtosecond LA-ICP-MS and FGS02 provided greater accuracy for ns-LA-ICP-MS. Statistically, nanosecond LA-ICP-MS with quantification by FGS02 and use of an internal standard provided the best overall accuracy. This observed accuracy for nanosecond LA-ICP-MS is possibly due to the fact that the values used for quantification are 4-5 times higher in concentration in FGS02 than FGS01 and thus higher than the expected concentration for NIST 1831, meaning that this difference in concentration helps to account for the increased negative bias associated with using another standard at a concentration closer to the expected value, such as with FGS01. The best results for femtosecond LA-ICP-MS in terms of accuracy were obtained when a more similar and matrix-matched standard was utilized for the quantification of NIST 1831 (i.e. FGS01), thus supporting the idea of matrix-matched and internal standard dependence for femtosecond LA-ICP-MS for the analysis of glass.

Table 7. Quantification results for NIST 1831 using different calibration standards, femtosecond LA-ICP-MS, with*out* use of an internal standard.

	NIST 612			FGS01			FGS02		
element	mean	std.dev.	% bias	mean	std.dev.	% bias	mean	std.dev.	% bias
Mg	21188.21	3036.74	0.1	24015.63	3441.97	13.5	18858.30	2702.81	-10.9
Al	4873.29	683.73	-23.6	6270.28	879.72	-1.7	5250.83	736.70	-17.7
Ti	117.78	16.29	3.5	133.91	18.52	17.7	102.51	14.17	-9.9
Rb	6.07	0.78	-0.6	9.38	1.21	53.6	5.67	0.73	-7.2
Sr	77.45	9.90	-13.1	106.82	13.66	19.9	80.39	10.28	-9.8
Zr	28.60	3.51	-34.0	42.01	5.16	-3.1	30.88	3.80	-28.8
Ba	27.53	3.42	-12.6	37.25	4.62	18.2	28.76	3.57	-8.7
La	1.88	0.25	-11.2	2.68	0.36	26.3	1.88	0.25	-11.4
Ce	4.26	0.51	-6.0	5.99	0.72	32.2	4.09	0.49	-9.7
Nd	1.54	0.15	-9.1	2.11	0.21	24.6	1.57	0.15	-6.9
Hf	0.77	0.07	-29.4	1.19	0.11	9.2	0.89	0.09	-18.2

When comparing nanosecond and femtosecond LA-ICP-MS results, the precision was comparable for the elements under investigation (note Figure 5) with the majority of the values less than 5% for both nanosecond and femtosecond LA-ICP-MS. The observed differences by element are attributed to the instrumental performance for each ICP-MS, where given elements/isotopes may perform better on one or the other optimized LA-ICP-MS system.

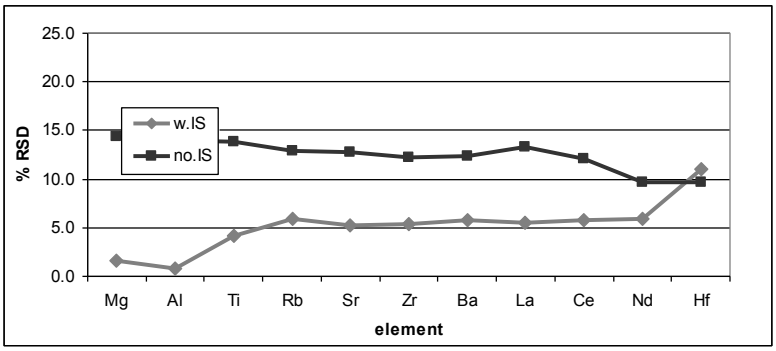

Figure 5. Precision results for NIST 1831 for femtosecond LA-ICP-MS, with vs. with*out* use of an internal standard.

2.4.2 Limits of Detection

When comparing limits of detection, it is evident that femtosecond LA-ICP-MS provided lower limits of detection, or greater sensitivity on the order of 2-7 times greater, per element than nanosecond LA-ICP-MS. A summary of the respective limits of detection can be found in Table 8. These lower limits of detection are attributed to the higher ablation efficiency (rate) for femtosecond laser ablation as well as ICP-MS performance, which is also correlated to smaller particle sizes; these advantages have been well documented in the literature [14, 20, 34-35]. Despite achieving higher limits of detection (lower sensitivity) than for nanosecond LA-ICP-MS, the stated limits of detection are still well below the concentrations found in typical float glass samples. The concentration ranges for the samples analyzed in this study are provided in Table 8 and validate the previous statement and support the recommended use of nanosecond LA-ICP-MS in the analyses of glass samples recovered at crime scenes. Although lower detection is not needed for this matrix (glass), it should be noted that if lower detection limits are necessary, femtosecond laser ablation can assist in achieving greater analyte sensitivity, potentially even for other matrices of forensic interest.

Table 8. Method detection limits, nanosecond (ns) and femtosecond (fs) LA-ICP-MS, respectively, all represented values are in units of ppm.

element	ns-LA-ICP-MS	fs-LA-ICP-MS	analyte range
Mg	2.88	1.13	23785.50 - 28717.68
Al	1.34	0.71	433.34 - 3937.77
Ti	3.03	0.54	49.95 - 428.52
Rb	0.14	0.04	0.48 - 4.46
Sr	0.05	0.01	20.77 - 89.02
Zr	0.13	0.02	20.62 - 222.75
Ba	0.32	0.05	5.57 - 38.71
La	0.05	0.01	1.17 - 2.48
Ce	0.05	0.01	1.94 - 4.65
Nd	0.21	0.04	0.69 - 2.24
Hf	0.14	0.05	0.44 - 5.74

2.4.3 Discrimination

In terms of discrimination power, both nanosecond and femtosecond LA-ICP-MS with use of an internal standard provided comparable discrimination (at the 95% confidence interval) for the glass casework sample set used in this study. More specifically, it was determined that all of the possible pairs (55) could be distinguished from each other when using the discrimination capabilities of all the selected elements combined. A summary of the discrimination results, in terms of the number of indistinguishable pairs and percent discrimination, by element can be found in Table 9. For illustrative and comparative purposes, all elements are shown despite the fact that only three elements (Ti, Sr, and Zr) were necessary to discriminate the glass set by both nanosecond LA-ICP-MS and femtosecond LA-ICP-MS, respectively.

Table 9. Discrimination results, nanosecond and femtosecond LA-ICP-MS, with and with*out* use of an internal standard, 55 possible sample comparisons.

	ns-LA-ICP-MS (with IS)		ns-LA-ICP-MS (no IS)		fs-LA-ICP-MS (with IS)		fs-LA-ICP-MS (no IS)	
element	No. pairs indistin.	percent discrim.	No. pairs indistin.	percent discrim.	No. pairs indistin.	percent discrim.	No. pairs indistin.	percent discrim.
Mg	54	1.8	53	3.6	23	58.2	12	78.2
Al	24	56.4	34	38.2	6	89.1	20	63.6
Ti	15	72.7	21	61.8	12	78.2	11	80.0
Rb	32	41.8	37	32.7	22	60.0	27	50.9
Sr	7	87.3	23	58.2	10	81.8	10	81.8
Zr	6	89.1	17	69.1	2	96.4	7	87.3
Ba	16	70.9	19	65.5	6	89.1	9	83.6
La	26	52.7	34	38.2	17	69.1	16	70.9
Ce	22	60.0	27	50.9	15	72.7	14	74.5
Nd	36	34.5	32	41.8	16	70.9	17	69.1
Hf	12	78.2	22	60.0	5	90.9	9	83.6
combined	0	100.0	3	94.5	0	100.0	0	100.0

Although the same conclusion was reached (100% discrimination) for both systems when using an internal standard, the discrimination power per element was much better for nanosecond LA-ICP-MS, with the exception of Sr where nanosecond provided 6.5% better discrimination power. This concept is especially noticeable for some of the more trace elements in the element menu (i.e. Rb, La, Ba, and Nd) which had considerable more discrimination power with femtosecond LA-ICP-MS. This observed increased discrimination is a result of the better sensitivity (lower detection capabilities) observed for femtosecond LA-ICP-MS (see Table 8), which resulted in increased precision and hence more discrimination potential.

The samples were also compared without use of an internal standard. Due to the lack of precision (higher %RSDs) observed for nanosecond LA-ICP-MS, the discrimination power per element was on the order of approximately 2-3 times less. In addition, discrimination analysis combining all elements by nanosecond LA-ICP-MS (without internal standard) yielded 3 indistinguishable pairs. The said samples found indistinguishable were not from the same source and did not originate from the same manufacturing plant at about the same time period, therefore not utilizing an internal standard resulted in a Type II error (false inclusion). From a forensic standpoint, committing this type of error should be avoided, which stresses again the importance of using an internal standard for nanosecond LA-ICP-MS glass analyses. For femtosecond LA-ICP-MS without use of an internal standard still provided 100% discrimination, which is remarkable considering the slightly higher degree of imprecision associated without use of an internal standard. As stated, besides having a high degree of variation (or at least detectable variation) with respect to the elemental profiles of the samples being compared, the other major contributing factor for sample discrimination studies will always be sample precision. The precision was superior across the sample replicates for femtosecond LA-ICP-MS (in most cases values < 5% RSD were obtained) even for quantification without use of an internal standard.

The precision across the sample set for both nanosecond and femtosecond LA-ICP-MS (for elements Ti, Zr, and Sr) is illustrated in Figures 6 and 7, these figures demonstrate how similar the precision obtained for both systems was when an internal standard was utilized during quantification.

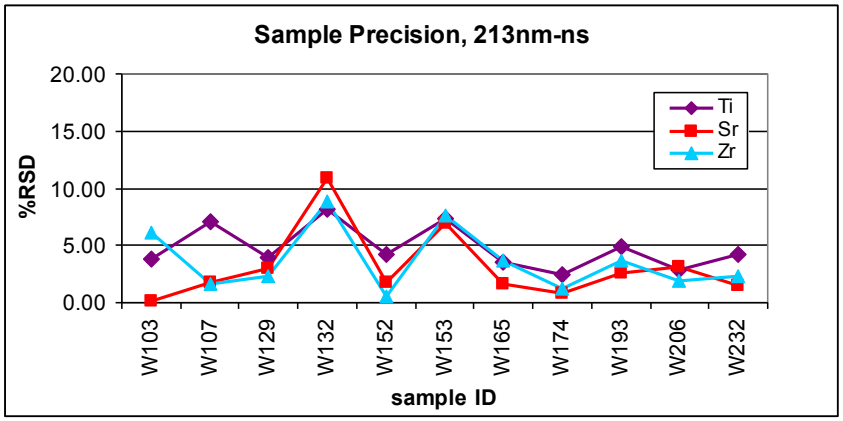

Figure 6. Sample precision (with respect to elements Ti, Sr, and Zr) for nanosecond LA-ICP-MS across the casework glass set used for discrimination assessment.

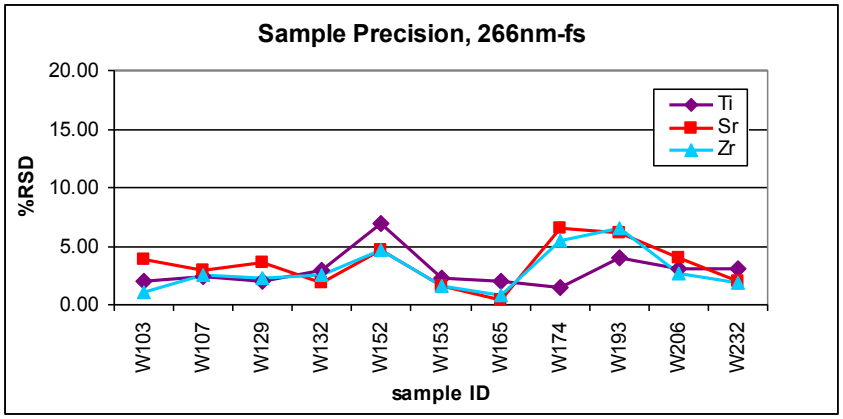

Figure 7. Sample precision (with respect to elements Ti, Sr, and Zr) for femtosecond LA-ICP-MS across the casework glass set used for discrimination assessment.

This observed precision for the sample set is different when compared to the precision observed for the 9 replicates analyzed for NIST 1831, where precision values for femtosecond LA-ICP-MS without use of an internal standard were between 10–15% RSD. This can be explained by looking to the analysis sequence itself. Breaking down the 9 replicates into groups of three (three replicates of NIST 1831 were analyzed at the beginning, mid, and end of the sequence), the precision of each group is comparable to that observed for both the samples by femtosecond LA-ICP-MS without use of an internal standard and to the precision found for the 9 replicates of NIST1831 when using an internal standard (where the precision was < 5% per element). Therefore, when sample replicates are run concurrently, as was the case for the discrimination study, it is apparent

that good precision can be obtained when an internal standard is not utilized for femtosecond LA-ICP-MS thus leading to a higher degree of discrimination potential. However, the accuracy of the respective measurements is less (note the analysis of NIST 1831) wherein the comparison values are then subject only to the analytical signal (not normalized to an internal standard), which can fluctuate over time. Thus, comparisons of samples over different days or even over the course of a single day would be inaccurate and thus lead to a potential increase in Type I and Type II errors. Therefore, it is recommended that use of an internal standard when quantifying and comparing glass samples even for femtosecond LA-ICP-MS.

As an illustration to demonstrate the similarities in the data used to discriminate the casework samples by nanosecond and femtosecond LA-ICP-MS, the % compositions per sample are shown in Figures 8 and 9. It can clearly be seen that almost identical elemental profiles were observed for each of the 11 casework samples for nanosecond and femtosecond LA-ICP-MS, respectively when using an internal standard for quantification purposes. Although illustratively plotted here in % (with 100% equivalent to the three elemental percentages combined), the actual composition of these elements is in the low to mid parts per million range. Hence, overall from precision to accuracy to discrimination potential, similar results were obtained for femtosecond and nanosecond LA-ICP-MS when using an internal standard and an appropriate quantification standard.

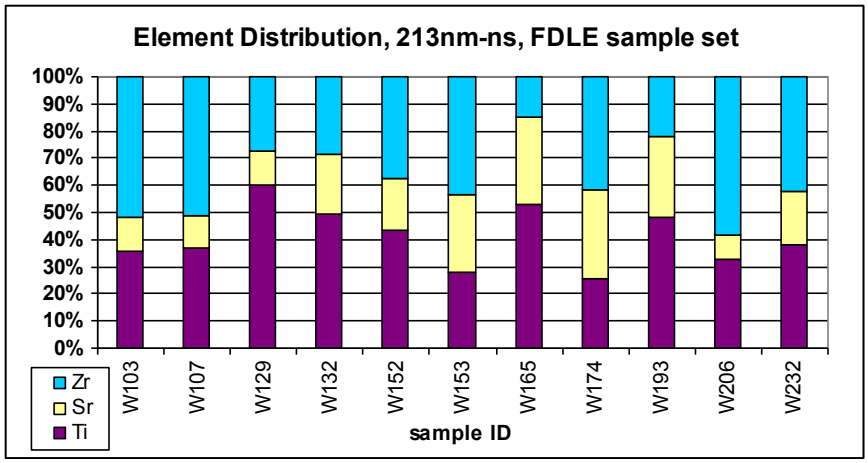

Figure 8. Elemental distribution (three elements) for nanosecond LA-ICP-MS across the casework glass sample set used for assessing discrimination power.

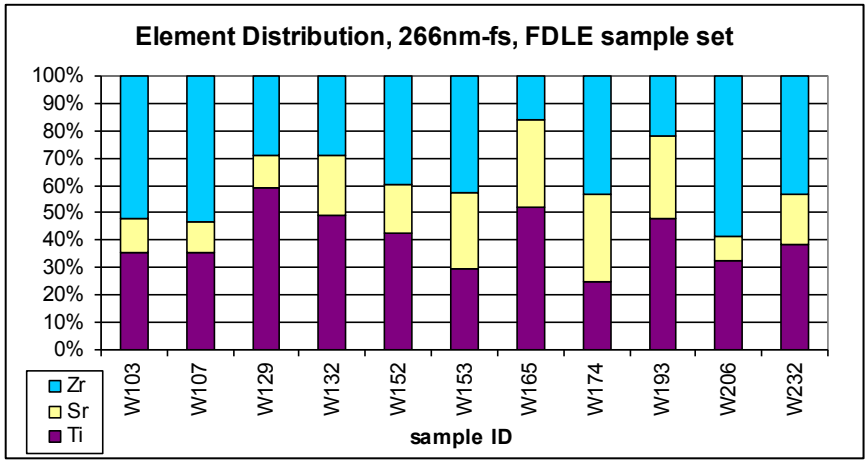

Figure 9. Elemental distribution (three elements) for femtosecond LA-ICP-MS across the casework glass sample set used for assessing discrimination power.

2.5 Conclusions

Two different LA-ICP-MS systems, a nanosecond (ns) LA-ICP-MS and a femtosecond (fs) LA-ICP-MS, were utilized for quantitative analysis of float glass standard reference material (NIST 1831). Three quantification approaches were compared (SRM NIST 612 and reference glasses FGS01 and FGS02 as calibrators) with and without the use of an internal standard (^{29}Si). Nanosecond LA-ICP-MS and femtosecond LA-ICP-MS were compared in terms of figures of merit important to any analytical method (accuracy, precision, and limits of detection) and for forensic cases, discrimination power. The results demonstrate that the use of an internal standard is necessary for most of the elements analyzed. In terms of accuracy and precision, nanosecond LA-ICP-MS and femtosecond LA-ICP-MS provided comparable results for the quantification of NIST 1831. The greatest accuracy when quantifying NIST 1831 was obtained when reference glasses FGS02 for nanosecond LA-ICP-MS and FGS01 fro femtosecond LA-ICP-MS, respectively, were used. These particular quantification standards are more matrix-matched to NIST 1831 (and to float glass samples collected from crime scenes) than NIST 612, ultimately meaning that accuracy for both nanosecond and femtosecond LA-ICP-MS is dependent on the quantification approach used.

Nanosecond LA-ICP-MS had higher detection limits (lower sensitivity) than femtosecond LA-ICP-MS where limits of detection were on the order of 3-10 times lower. Nevertheless, detection limits for nanosecond LA-ICP-MS were well below the typical concentrations found in glass samples collected from most crime scenes. Thus, lower detection limits achieved by femtosecond LA-ICP-MS did not provide any additional advantage over ns-LA-ICP-MS in this case. Femtosecond LA-ICP-MS also yielded slightly better discrimination power per element (~ 2-3% more discrimination when compared to nanosecond LA-ICP-MS). However when all the casework samples were compared using a combination of all 11 elements in the detailed method (and representing major, minor, and trace elements), both nanosecond and femtosecond LA-ICP-MS were able to discriminate all of the 55 possible pairs (100% discrimination). Due to less precision associated for the quantified forensic glass sample replicates when an internal standard was not used, three pairs were found indistinguishable for nanosecond LA-ICP-MS that should have been discriminated. Therefore, evidence of Type II error (false inclusion) existed. Femtosecond LA-ICP-MS without the use of an internal standard and combining all elements for discrimination also provided 100% discrimination power. However, it is more likely that Type I and Type II errors would be increased when comparisons are made without use of an internal standard, particularly when samples are analyzed on different days. Thus, it is suggested that a quantification approach that employs an internal standard be utilized even for femtosecond LA-ICP-MS when analyzing glass samples.

Overall, nanosecond LA-ICP-MS and femtosecond LA-ICP-MS provided similar figures of merit. Therefore despite some advantages the additional cost of a femtosecond laser would be very difficult to justify for the analysis and comparison of glass in typical forensic laboratories.

3. LIBS FOR THE ELEMENTAL ANALYSIS AND DISCRIMINATION OF GLASS, A COMPARISON TO XRF AND LA-ICP-MS

3.1 Elemental Analysis of Glass by LIBS

Laser induced breakdown spectroscopy (LIBS) is a relatively new application for the forensic analysis of glass. However, in the last year three publications came out regarding the utility of this technique for forensic glass comparisons and each had a different approach (especially in terms data analysis). This short list includes some of the work presented in this report, which also appears in a publication regarding the discrimination potential of LIBS [36]. Research presented by Rodriguez-Celis et al who used linear and rank correlations to compare glass samples via use of entire spectra (and/or by masking parts of the associated spectra), it was concluded in this study that 100% identification of glass samples was achieved [37]. The other publication by Bridge et al who used LIBS to achieve 83% discrimination of glass samples used pairwise comparison analysis using element ratios [38], however, there was no mention of how Type I or Type II errors were dealt with (or even if they were tested for). In addition, Bridge et al used different detector gate delays which they say varied depending on the sample matrix, between 2.0μs to 6.5μs [38]; this large variation in the delay ultimately affects the spectra generated, such that different emission lines are present or absent (a dependence on plasma evolution characteristics). As a result, if samples are being compared for discrimination purposes, as they were in the referenced paper [38], it is absolutely necessary that all parameters remain constant in order to achieve the most accurate comparisons possible.

3.3 Methodology

3.3.1 Initial Remarks

This part of the report is comprised of the analysis of a float glass sample set by LIBS and the comparison of the generated discrimination results to two other leading elemental analysis techniques, XRF and LA-ICP-MS of which the same sample set was analyzed. Thus, the data presented in the following sections was a product of a collaborative effort amongst different research personnel, including XRF data acquisition and analysis by Scot Ryland at the Florida Department of Law Enforcement (FDLE),

sample collection (of the 41 glass sample set used for the comparison) and LA-ICP-MS data acquisition by Sayuri Umperiezz (a former master's student under Dr. Almirall), and LIBS data acquisition and analysis, assisted by Dr. Cleon Barnett (a former Post Doc in the Almirall laboratory). All the respective contributors had their input in the stated project and thus deserve credit for their contributions and, at times, their advisement as the results were being summarized and compared.

In addition to the comparison study already mentioned, some early LIBS results (and the methodology behind those results) has been included mainly because the results show some advantages of using dual pulse LIBS as versus single pulse LIBS that may be of use to those who may follow up on this work. At any rate, upon obtaining what was thought to be optimum parameters (obtained with a commercial LIBS system), the same 41 glass sample set (under investigation in the comparison study) was analyzed and the results were far less than stellar when compared to say LA-ICP-MS. Therefore, the methodologies and results from this early work were added simply as an illustration of the initial failures encountered and, more importantly, the great progress that was made with respect to handling of LIBS data for forensic glass comparisons. At any rate, the addition of this data was not intended for confusion, rather the intention is that the two separate LIBS methods and results are well distinguished. The early work has been characterized (and subsequently marked) as LIBS (Early Crossfire Studies) while the most recent LIBS methods and results are simply called just LIBS, hopefully this will help reduce such potential confusion.

3.3.2 Instrumentation

3.3.2.2 LIBS

3.3.2.2.1 LIBS Principles and Considerations

Although laser induced breakdown spectroscopy (LIBS) has been around for a long time, physicists have been using LIBS for years for theoretical studies, the technique as an analytical chemistry tool is relatively new. LIBS is one of the many analytical methods that fall under the category of atomic emission and is rapidly becoming popular, especially in the realm of analytical research and the potential success of commercialization.

In brief, during a LIBS experiment, a laser to sample interaction causes an emission of light from the sample surface (this emission is characteristic of the composition of the sample). This emitted light can then be collected via a basic optical spectrometer, which translates the captured light into an emission spectrum, which ultimately can be used for characterization purposes.

More specifically, in typical LIBS experiments, a high powered laser is focused onto a sample surface, within picoseconds free and loosely bound electrons in the sample matrix interact with the laser pulse [16, 39-40]. The pulse width for LIBS is typically in the ~3-5ns range for reasons that will become evident as the processes are described. The electron interaction with the laser pulse occurs through inverse bremsstrahlung processes as additional electrons (from the sample) are emitted/ejected via energetic collision. This process (or ionization cascade) repeats and repeats, with the free electrons absorbing energy from the laser pulse, which then cause additional collisions and in turn cause additional electrons to be emitted from the sample matrix, until a thermally hot laser induced plasma evolves from the sample surface [16]. Plasma evolution into the microsecond time scale results electronic and ionic recombination, which causes the plasma to cool and eventually extinguish as the molecules and atoms relax from the excited state down to the ground state. This relaxation step is characterized by a wealth of atomic, ionic and even molecular emission lines, which in turn can help determine sample composition and thus makes analytical chemistry possible [16, 39-40].

3.3.2.2.2 Advantages of LIBS

A LIBS setup is fairly simple, less complex, and rather inexpensive compared to its distant relative, laser ablation. The major components of a LIBS system includes a laser source (or multiple laser sources for dual pulse setups), a spectrometer equipped with a fiber optic cable, a set of optics to deliver the laser pulse and capture the emitted light, and a device (computer or delay generator) to control and synchronize the triggering of the laser and spectrometer, respectively. Multiple emission events in conjunction with the generated laser induced plasma at each laser pulse interval can be captured spectrally and stored in a relatively short period of time. So sample throughput

is high, actually it takes more time to qualitatively analyze a given spectrograph than it does to collect it.

3.3.2.2.3 Disadvantages of LIBS

The drawbacks for LIBS include higher degrees of imprecision (% RSDs typically > 10%), higher limits of detection (in the ppm range) [39], and those issues that are just grouped together due to the "infancy" of the technique, wherein data analysis and the analytical approach is still under development in order to achieve the best optimization parameters and comparable discrimination power. In addition, a flat sample surface for LIBS analyses is often necessary to ensure optimum laser to sample interaction and optimal detection, this is especially important when making sample comparisons. Nonetheless, this can be countered simply by the utilization of a pliable mounting media, as long as from a forensic standpoint that mounting media (i.e. clay) does not contaminate the sample. And, in relation to that, slightly larger sample sizes due to sample destruction may be necessary in comparison to laser ablation, especially in the case where a laser operating at 1064nm (~100mJ) is utilized, which results in a considerable amount of surface damage in comparison to a UV laser (at maximum energy).

3.3.2.2.4 Figures of merit for LIBS, XRF and LA-ICP-MS

Despite the disadvantages mentioned in the last section, the instrumentation is comparatively inexpensive in relation to the more mature analytical techniques of XRF and LA-ICP-MS. In addition, LIBS is less complex to operate, it has the capability for portability, and the analyst can generate large quantities of data over a short period of time (a rapid approach to elemental analysis). In this chapter, LIBS will be compared to the aforementioned analytical methods (XRF and LA-ICP-MS), a general comparison of these three techniques can be found in Table 10.

Table 10. Figures of merit comparison for LIBS, XRF and LA-ICP-MS. Some details adapted from [3].

Parameter	XRF	LA-ICP-MS	LIBS
Operating Principle	Highly energetic X-rays knock out an inner shell electron. Relaxation of an outer shell electron into the vacant position causes emission of characteristic X-rays	Laser photons remove material from sample. Submicron-sized particles are transported into the ICP which atomizes and ionizes the ablated material; ions are detected by MS	Laser photons induce matrix breakdown at sample surface. Characteristic emission lines are produced in the UV, VIS, and near IR range
Accuracy	Semi-quantitative	Quantitative	Semi-quantitative
Precision	Fair – good (5-10% RSD)	Excellent (< 5% RSD)	Fair – good (5-20% RSD)
Sensitivity	100 ppm	< 1 ppm	10 - 50 ppm
Discrimination	Very good - excellent	Excellent	Good – very good
Complexity	Easy to use	Difficult to use	Very easy to use
Sample Consumption	Nondestructive	Almost nondestructive	Almost nondestructive
Throughput	~30 min / analysis	~3 min / analysis	~30 sec / analysis
Cost	~ $120,000	~ $210,000	$50,000 - $150,000

3.3.2.3 LIBS Systems Descriptions

3.3.2.3.1 LIBS (Early Crossfire Studies)

The very first (version 1) Photon Machines Crossfire LIBS system (San Diego, CA), which has since been commercialized, was part of what would become the LIBS lab. The particular device, which has since been replaced by version 2, was developed with the intention to make LIBS measurements easier and thus wouldn't require the user to have a wealth of knowledge regarding the use of and positioning of optics and how to control timing functions (laser and detector), etc. The Crossfire instrument has a camera to view the sample and a software program that allowed the operator to basically control everything. Nevertheless, this first prototype of a commercial instrument was not user friendly at the time but many improvements from this manufacturer and from others that we have worked with throughout this project (a total of 4 different manufacturers provided instrumentation for our evaluation during this project period, Photon Machines, Foster and Freeman, Applied Spectra and Ocean Optics). Version 1 of the Photon Machines instrument became a work in progress where oftentimes it took manipulation of

the optics and creation of special devices to position parts like the fiber optic cable to make spectroscopic measurements.

The initial Crossfire had the capability of doing single, dual, and even triple pulse LIBS experiments. Data with respect to (and comparison thereof) the former two types of experiments (single and dual pulse) can be found in the results and discussion section. Nonetheless, the components and parameters by which spectral analysis was conducted with the Crossfire can be found here. This system was equipped with two Q-switched Nd:YAG lasers: a New Wave Research Tempest laser (Fremont, CA) operating at 266nm (with a pulse width of 3-5ns, ~25mJ energy per pulse) and a New Wave Research Solo PIV laser (Fremont, CA) operating at 1064nm (3-5ns pulse width, ~100mJ) situated orthogonal to the UV laser. An Andor Mechelle 5000 Spectrometer equipped with an ICCD, with a spectral range of 200-950nm and a resolution of R=5000, was utilized for spectroscopic measurements. More details concerning the equipment above can be found in the next section.

For the single-pulse experiment, the 266nm laser was utilized at full energy and the laser was fired at a 1 Hz repetition rate, the gate delay on the spectrometer was 1μs with a gate pulse width of 10μs, and a total of 10 spectra were accumulated (which coincided with 100 laser shots. The fiber optic cable was manually positioned at a 45° angle (to the sample surface) and argon was used, which had previously been determined to provide signal enhancement. For the dual pulse experiment, the same parameters were utilized with the exception of the gate delay, which had to correlate to the second pulse (IR, 1064nm) fired orthogonal to the first pulse (UV, 266nm) at a 0.5μs delay; thus, the detector delay was set at 1.5μs to capture the plasma reheating and hence signal enhancement.

3.3.2.3.2 LIBS

Experiments were conducted using a custom LIBS system constructed at FIU by a former post doc in our lab, Dr. Cleon Barnett. This system was equipped with a New Wave Research Q-switched Nd:YAG Tempest laser (Fremont, CA) operating at 266nm and a pulse width of 3-5ns (full width half maximum), which was chosen for this analysis due to an observed improved laser-to-sample interaction with glass and thus improved

precision (as versus the laser typically used for LIBS analyses, 1064nm) [58, 61]. A 3X beam expander was utilized to enlarge the beam diameter to approximately 11mm. The laser beam was then focused perpendicular to the sample surface using a plan-convex lens with a focal length (f) of 150mm. Laser energies of ~25mJ per laser pulse and a spot size of approximately 190µm remained constant throughout the analytical sequence and all LIBS analyses were conducted under atmospheric pressure in air. Light (emission) from the laser induced plasma was imaged from the side (parallel to the sample surface or 90° in relation to the laser beam being fired) by a pair of plano-convex lenses (f=75mm) which focused and transmitted the laser induced plasma emission into an optical fiber that had a diameter of 50µm. This fiber was coupled to the entrance slit of an Andor Mechelle 5000 spectrometer (South Windsor, CT) equipped with an Andor iStar Intensified Charge Coupled Device (ICCD), which converted the image of the light being emitted at laser to sample interaction into a spectrograph. The spectral range collected for each sample ranged from 200-950nm with a resolution of ~5000. The repetition rate for the spectrometer was set at 0.67Hz, at this repetition rate the spectrometer could capture a complete set of data (full spectrum) for each laser shot. Both the laser flashlamp and the Q-switch were externally controlled using a Berkeley Nucleonics' Model 565 Delay Generator (San Rafael, CA), which allowed for all signals being sent by each of the respective devices to be in sync in conjunction with the optimized program. The emission lines generated by the laser induced plasma were accumulated at a 1.2µs delay upon plasma ignition with an integration width of 3.5µs. The term accumulated in the previous sentence means that all the acquired spectra were added together to arrive at one cumulative spectrum, although software did permit the analyst to look at each of the spectra in that accumulated signal if warranted. A schematic of the LIBS setup utilized for this part of the study can be found in Figure 10.

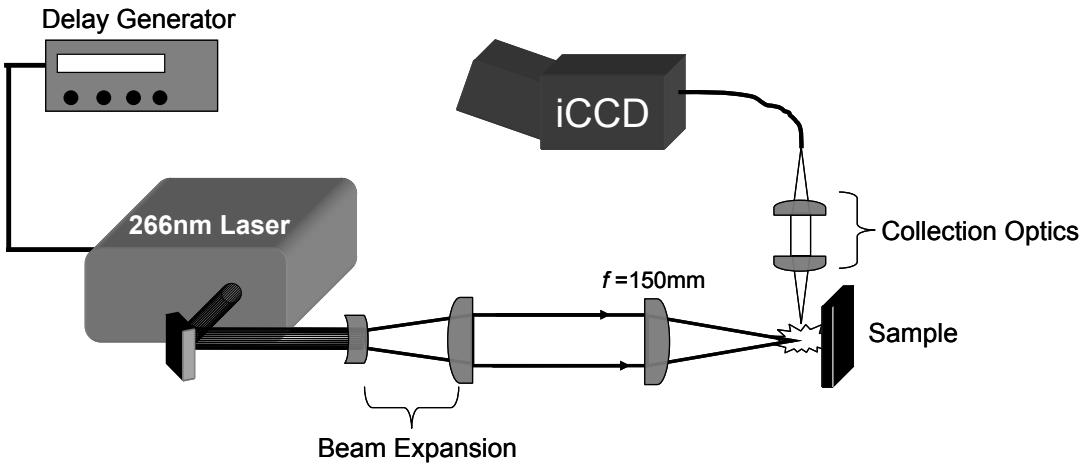

Figure 10. Experimental setup for LIBS measurements. iCCD stands for intensified charge-coupled device and f is the focal length.

3.3.1.4 XRF Principles and Considerations

Since this chapter of the report primarily deals with the forensic analysis of glass by LIBS and its comparison to the two leading techniques used in forensic labs for elemental analysis, LA-ICP-MS and what this section encompasses X-ray fluorescence (XRF), only a few statements will be made regarding the theory behind XRF since this information can also be found elswhere [26]. XRF sample excitation is brought about by focusing an X-ray beam onto the sample surface, absorption of the primary beam causes relaxation and elements will emit their own characteristic X-rays which are typically captured by an energy dispersive detector where simultaneous detection of multiple element is possible [26]. Most applications involve the utility of XRF for qualitative purposes, although semi-quantitative and quantitative analyses are possible when matrix-matched standards are available. The main disadvantages include larger sample size requirements (than LA-ICP-MS and possibly LIBS depending on the laser utilized) and the necessity of having a flat surface for proper XRF analyses. The main advantage and its attraction to forensic labs is that XRF is a nondestructive technique that can be used for many types of analyses (i.e. forensic paint examinations) [3].

3.3.2.5 XRF System Description

An EDAX Eagle Micro X-Ray Fluorescence Spectrometer (Mahwah, NJ) equipped with a rhodium X-ray tube was utilized for this part of the study. The instrument was operated with a 40kV excitation potential, a 17μs time constant, and 40-45% dead time. Other instrumental parameters for the stated device included a 300μm diameter focusing capillary and 1200s of live count time. The sample chamber was operated under low vacuum conditions. For the remainder of this report μXRF will be represented as just XRF.

3.3.2.6 LA-ICP-MS Principles and Considerations

The background information stating the principles behind and utility of LA-ICP-MS for forensic glass analyses was covered in the previous chapter. Therefore, please see those respective sections for more detail with respect to chemical analysis by LA-ICP-MS.

3.3.2.7 LA-ICP-MS System Description

A New Wave Research UP213 Laser Ablation system (Fremont, CA) coupled to a Perkin Elmer ELAN 6100 DRC II ICP-MS (Waltham, MA) was used for the LA-ICP-MS part in this study as well. The parameters, including the ICP-MS conditions, can be found in the last chapter in Table 1. For ease of reference, however, the laser equipped in the ablation system was a Nd:YAG (4 ns) Q-switched laser operating at 213nm and 100% energy (27.2 J/cm^2 fluence). Single spot ablation mode was used with a spot size of 55μm and a repetition rate of 10Hz, the time length for sampling was 60sec. Helium with a flow rate of 0.9 L/min was the carrier gas into and from the ablation chamber, the carrier gas then coupled to argon (1 L/min) prior to entering the ICP. The ICP-MS parameters included an RF power of 1500W, a plasma gas (argon) flow rate of 16 L/min, an auxiliary (argon) flow rate of 1 L/min, and a dwell time of 8.3 ms.

3.3.3 Sample Descriptions

3.3.3.1 Glass Standards

Standard reference materials NIST 612 and NIST 1831 were utilized for optimization of each of the aforementioned instrumental setups (LIBS, XRF, and LA-ICP-MS). These two standard reference materials were used either for direct optimization, quantification, or for quality control purposes. More specifically, the standards were used for optimization and quality control measures for LIBS and XRF.

For LA-ICP-MS analyses, NIST 612 was used as an external calibration source ultimately for quantitative analysis of the glass sample set while NIST 1831 was used as a calibration verification sample (second source check standard) to ensure optimum accuracy and precision across the given sample sequence.

3.3.3.2 Glass Sample Set

The sample set of interest in this study was comprised of 41 different automotive glass fragments extracted directly from 14 different vehicles located in junkyards in and around Miami, FL. The respective glass sample set included seven side window fragments, 6 rear window fragments, and 28 windshield fragments (14 inside windshield and 14 outside windshield samples) all which came from automotive vehicles produced between the years of 1995 and 2005. The non-float surfaces of the respective glass samples were examined via each of the three analytical techniques (LIBS, XRF, and LA-ICP-MS).

3.3.4 Data Analysis

3.3.4.1 LIBS (Early Crossfire Studies)

Sample replicates were analyzed by accumulating 10 LIBS spectra into one spectrum (a feature of the spectrometer), with three replicates per sample. Further data reduction was performed using Origin software (OriginLab Corporation, Southampton, MA) wherein peak selection occurred and the associated intensities were transferred into an Excel spreadsheet where means, standard deviations, and %RSDs were tabulated.

Peak selection included the following emission lines: 285.5nm (Mg), 317.9nm (Ti), 407.7nm (Sr), 445.5nm (Ca), and 646.3nm (Fe), and these were chosen based on presence in the samples and associated peak presence when NIST 1831 was analyzed (for verification purposes). Other factors that influenced the selection of these particular lines included peak shape and what appeared to be variation in intensities across the sample set. These peak intensities (correlated to an element) were then ratioed to each other, which increased the precision of the sample replicates. Thus, all ten possible ratios were used for discrimination purposes, the list included: Ti/Fe, Mg/Fe, Ti/Ca, Ca/Sr, Fe/Sr, Ti/Sr, Ca/Mg, Ti/Mg, Ca/Fe, and Mg/Sr. The same discrimination protocol mentioned

earlier was followed (namely, ANOVA with Tukey's honestly significance test, at the 95% confidence interval).

3.3.4.2 LIBS

Each sample replicate LIBS spectrum was collected as a result of accumulating spectra for 50 laser shots. After each spectrum was acquired, the sample was rotated to a new spot for a total of 5 spots or replicate analyses per sample. Twenty-two (22) peaks/emission lines were initially chosen for data analysis based on their presence across all 41 glass samples; the selected peaks included 9 different elements, Al, Ca, Fe, K, Mg, Na, Si, Sr, and Ti. Both peak intensities (peak heights) and peak areas (via integration) were evaluated statistically with respect to the sample replicates; it was observed that peak areas provided greater precision when compared to just using peak heights or intensities. Since precision is an important factor in discriminating samples, peak areas were utilized for further data reduction purposes. From the 22 peak areas detailed above, every possible ratio was performed and compared with respect to discrimination potential; this resulted in 231 possible ratios [N(N-1)/2 where N is the number of peaks].

Since extensive work was conducted with respect to determining the optimum data analysis approach for glass data generated with the LIBS setup, the steps taken and the reasoning behind the final discrimination approach will be discussed in part here and then finished in the Results and Discussion section. In brief (and somewhat of a prelude of things to come), discrimination for each individual ratio was conducted on the 41 glass set using a student t-test at the 95% confidence interval to coincide with the confidence intervals utilized for LA-ICP-MS and μXRF and thus make the comparison between techniques more valid. A program was created by my colleague Dr. Cleon Barnett using Mathematica (Wolfram Research, Champaign, IL), which greatly assisted with many of the determinations made with respect to how to best analyze and efficiently analyze LIBS data for discrimination of glass samples.

One of the most important steps in determining what protocol for LIBS data analysis for glass comparisons should be followed was the utility of a 42nd sample fragment as a quality control measure. This sample was the same sample analyzed twice during the analytical sequence, once towards the middle of the run and again at the end,

and thus the elemental composition was exactly the same as a previous sample. The sample duplicate was treated as an individual sample throughout the entire analytical approach and was then used to eliminate ratios that provided a false exclusion (or Type I error), meaning that the same sample was discriminated when it came from the same source of origin. Based on this factor, 146 ratios (out of 231) gave a false exclusion whereas 85 ratios made the accurate conclusion, namely that the same sample was found indistinguishable.

Of these 85 ratios, 10 were selected based on their respective degrees of discrimination; note that associated ratios were not repeated [i.e. 394.4nm/460.7nm (Al/Sr) and 460.7nm/394.4nm (Sr/Al)] despite having equivalent and/or greater discrimination power than a non-associated ratio. These 10 ratios and their individual discrimination results are reported in Table 11. The final step in this approach was to limit the number of ratios utilized for discrimination to only 6 ratios (of the 10) in combination in order to remain consistent with the number of ratios used to discriminate the sample set by XRF, which was also 6.

Table 11. The ten ratios used for discrimination of the glass sample set by LIBS.

#	peak ratio	description	# indist.pairs	% discrimination
1	394.4nm / 330.0nm	Al/Na	70	91.5
2	766.5nm / 643.9nm	K/Ca	84	89.8
3	394.4nm / 371.9nm	Al/Fe	86	89.5
4	438.4nm / 766.5nm	Fe/K	90	89.0
5	534.9nm / 766.5nm	Ca/K	91	88.9
6	371.9nm / 396.2nm	Fe/Al	91	88.9
7	766.5nm / 645.0nm	K/Ca	93	88.7
8	394.4nm / 460.7nm	Al/Sr	104	87.3
9	460.7nm / 766.5nm	Sr/K	104	87.3
10	818.3nm / 766.5nm	Na/K	141	82.8

3.3.4.3 XRF

Five replicate analyses were performed on each glass fragment in the 41 glass sample set with a sampling target area defined by the 300μm diameter X-ray spot. The element menu consisted of six elements (K, Ca, Ti, Fe, Sr, and Zr) and respective peak intensities were acquired per element for each sample. Taking these sample peak intensities, further data reduction was conducted where the element intensities were

subdivided into six element ratios (Ca/Fe, Sr/Zr, Ca/K, Fe/Zr, Fe/Sr, and Fe/Ti) to be used for sample comparison/discrimination purposes. The intensities of the K alpha peaks corresponding to each of the respective elements were determined following background subtraction utilizing peak deconvolution and generation software. These particular element ratios are routinely used for glass casework examinations at FDLE and are the product of many years of experience and discrimination studies conducted by Scott Ryland at FDLE. In addition, the match criteria used routinely at FDLE is a three sigma criterion, which was followed for all sample (pairwise) comparisons by XRF. More specifically, the three sigma rule characterizes a sample (via the ratios mentioned earlier) based on the mean value (of all the sample replicates) ± three times the standard deviation. If a collective sample ratio overlapped with another sample ratio, then the two pairs were declared to be indistinguishable by the three sigma criterion. If there was no statistical overlap between two sample signals (or ratios in this case) then the samples were discriminated. At any rate, the pairs found indistinguishable were subjected to a t-test at the 95% confidence interval and some pairs within the sample set were further discriminated (thus reducing the amount of indistinguishable pairs and increasing the percent discrimination for that approach).

3.3.4.4 LA-ICP-MS

Three replicates (pertaining to different sampling or ablated spots) for each sample were analyzed by LA-ICP-MS. The element menu for this technique included five isotopes chosen due to their excellent discrimination power: ^{49}Ti, ^{85}Rb, ^{88}Sr, ^{90}Zr, and ^{137}Ba with ^{29}Si used as the internal standard. The quantification of each elemental concentration was calculated using Glitter software (Macquarie Ltd, Australia), where a single point calibration source (NIST 612) and the internal standard (^{29}Si) were used to convert intensity (counts per second) via integration of time-resolved spectra into concentration (in ppm). The resulting elemental concentrations were then used to characterize the given samples and ultimately to associate two glass fragments (meaning indistinguishable or what forensic examiner's would call a match or "likely to have originated from the same source) or to discriminate a given glass fragment from another

fragment (meaning they are significantly different with respect to elemental composition).

The data analysis utilized for the LA-ICP-MS results included a combination of pairwise comparison analysis using ANOVA in Systat 11 (San Jose, CA) with Tukey's honestly significant different test (HSD). To the pairs found indistinguishable by pairwise comparison analysis a t-test at the 95% confidence interval was applied (via Microsoft Excel, Redmond, WA). Thus, a given pair found indistinguishable using the combination of the two data analysis strategies was ultimately determined indistinguishable, meaning the fragments have very similar (almost exact) elemental profiles.

3.4 Results and Discussion

3.4.1 LIBS (Early Crossfire Studies)

Upon acquisition of Photon Machine's multi-pulse capability device, work in the area of method development had to be performed prior to any actual sample analysis. The parameters addressed included the number of shots and acquisitions, the gate pulse width, the detector gate delay, argon pressure (or non-use), etc. Once a method was established for both single (UV, 266nm) and double pulse LIBS (UV, 266nm → IR, 1064nm), the glass sample set consisting of 41 automotive glasses was analyzed.

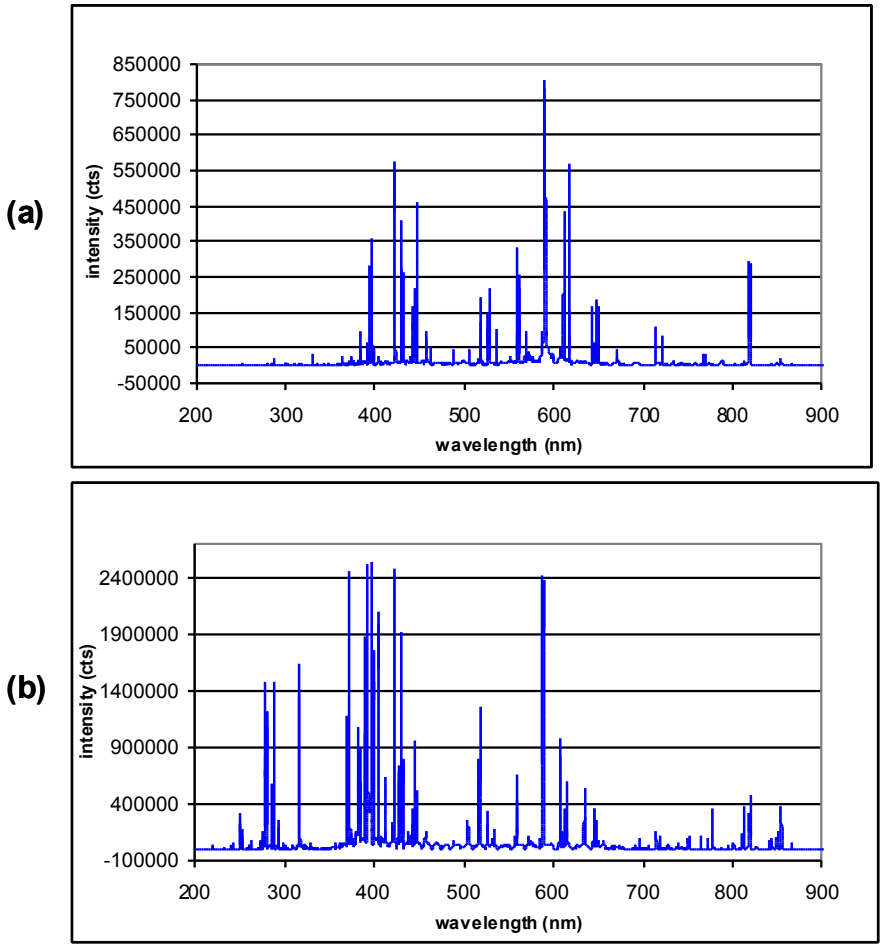

Figure 11. (a) Single pulse LIBS and (b) dual pulse LIBS spectra for a float glass sample.

Figure 11 shows the effects of dual pulse LIBS full spectrum, as compared to single pulse LIBS for sample 1 in the 41 glass sample set. Notice that in the dual pulse experiment [Figure 11(b)], the signal is enhanced by a factor of about 30, and more importantly the spectra is more "rich" (or abundant) in spectral lines. It is important to point out that the scaling on the y-axis (intensity) between Figure 11(a) and 11(b) is different so it may appear that some single pulse peaks are larger than the dual pulse experiment when they really are not. Not only does dual pulse LIBS provided greater sensitivity, but it also generates additional spectral lines that may (or may not) be helpful with sample characterization and ultimately discrimination. By expanding the baseline and overlaying the respective spectra (dual pulse spectra plus single pulse spectra) as in Figure 12, these differences and enhancement effects can be further visualized. More specifically, for the first spectra, see Figure 12(a) which depicts the region between

275nm and 300nm, with single pulse (UV, 266nm laser) there are very few peaks, most of which would be hard to discern from the background signal. However, when the dual pulse experiment was performed on the same sample, eight additional peaks in this specified region are now present. Figure 12(b) demonstrates signal enhancement by utilizing dual pulsed LIBS in comparison to the same peaks found for single pulse LIBS. Signal enhancement by dual pulse LIBS has been reported extensively in the literature [39].

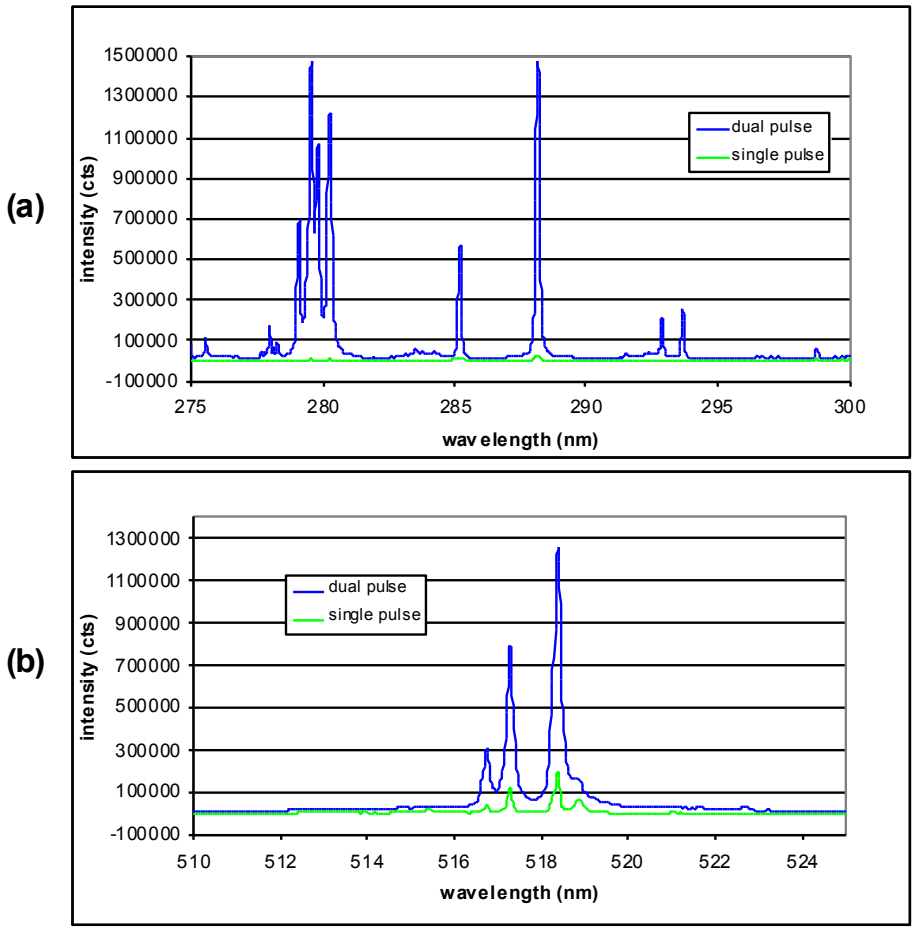

Figure 12. LIBS sample spectra demonstrating (a) the addition of more spectral lines and (b) signal enhancement of dual pulse LIBS.

Another variable studied and compared for these initial LIBS experiments was the variation between sample replicates or precision (across the 41 glass set). The dual pulse LIBS provided superior precision for the Sr line at 407.7nm over single pulse LIBS, which can be seen in Figure 13, and this same pattern was observed for the other

emission lines used in this study. Many of the said precision values are less than 10% RSD, which is considered to be good for LIBS analyses. Nevertheless, despite the observed improvement in precision for dual LIBS, the said values are still higher in magnitude to the precision of strontium (concentrations) obtained via LA-ICP-MS analyses. Considering the two techniques and the principles behind them, it would be remarkable if LIBS was able to achieve the low %RSDs typically acquired with LA-ICP-MS.

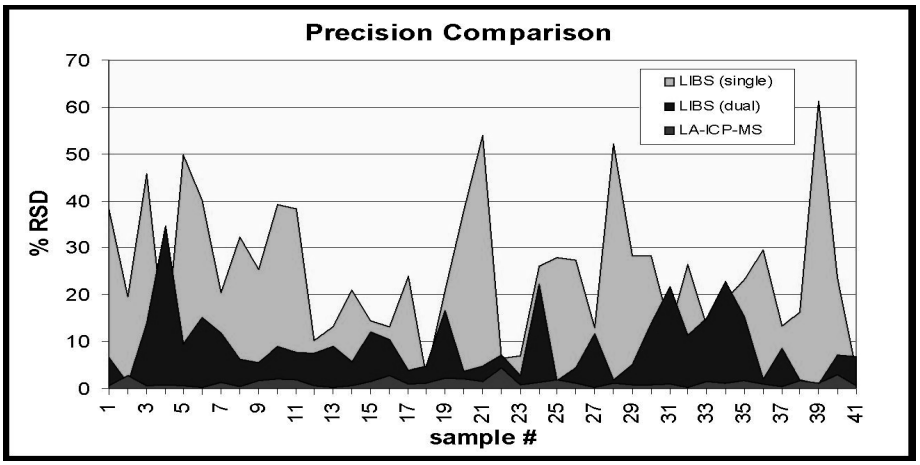

Figure 13. Precision comparison between single pulse LIBS, dual pulse LIBS, and LA-ICP-MS for strontium.

The gains made in precision by dual pulse LIBS were, nevertheless, overshadowed by the lack of discrimination power. Using all of the possible combinations of ratios, the number of indistinguishable pairs found was 385 out of a possible 820, which accounts for 53% discrimination power. Table 12 shows the discrimination results per element ratio utilized for pairwise comparison analysis. The large number of indistinguishable pairs encountered with this early discrimination study was discouraging at first glance, especially given the fact that the LA-ICP-MS results had already been tabulated (and came up with just 9 indistinguishable pairs by ANOVA).

Furthermore, the lack of discrimination power shown in this early experiment simply meant that the lines chosen were just not discriminating, and more importantly that a more advanced data analysis protocol was necessary to achieve competitive discrimination results when compared to other elemental analysis techniques. That was

the beginning of the extensive data analysis study for forensic glass analyses by LIBS and the data analysis protocol outlined in this report.

Table 12. Discrimination results per ratio, dual pulse LIBS.

element ratio	# indist.pairs	% discrimin.
Ca/Sr	459	44.0
Fe/Sr	466	43.2
Ca/Mg	627	23.5
Ti/Sr	637	22.3
Mg/Sr	657	19.9
Ti/Mg	665	18.9
Mg/Fe	672	18.0
Ti/Ca	753	8.2
Ca/Fe	757	7.7
Ti/Fe	763	7.0
combined	385	53.0

3.4.2 Discrimination (Comparison of LIBS, XRF, and LA-ICP-MS)

3.4.2.1 LIBS

All of the possible combinations of the 10 optimized ratios (using 6 different ratios in each combination) were assessed and further ranked in terms of discrimination power. In total, 210 different combinations {[n!/[(n-m)!m!] where n is the total number of ratios and m is the number of ratios used per discrimination (6)} were evaluated (i.e. 1,2,3,4,5,6; 1,2,3,4,5,7; etc); recall that at this point in the data evaluation process, the best discriminating ratios have been selected and the possibility of committing a Type II error (false exclusion) had been eliminated.

Of the 210 combinations, 60 of them provided inaccurate discrimination results; more specifically, these particular ratio combinations gave one or more false inclusions (Type I errors) whereby two samples were found to be indistinguishable that should have been discriminated. The reason why the said samples should be discriminated is because they originated from different vehicle makes and models which were consequently manufactured in different years. In the worst case scenario (combination #127), 9 indistinguishable pairs were found, 6 of which were false inclusions leaving 3 pairs that had explanation (and were valid associations). This particular combination would not be

used to discriminate glass samples; actually, none of the 60 combinations that produced false inclusions would be considered adequate for the discrimination of glass by LIBS.

Nevertheless, 150 combinations (of the possible 210) did provide accurate discrimination results, with no presence of Type I or Type II errors. The indistinguishable pairs found by these combinations were all explainable, meaning that they originated from the same vehicle and thus were likely produced in the same manufacturing plant during approximately the same time. The best case scenario in this category resulted in only 1 indistinguishable pair, sample 6 and sample 7, which are side and rear window fragments extracted from a 2004 Chevrolet Cavalier. Thirty-six different combinations concluded the same result, namely 1 indistinguishable pair (6:7). Interestingly, this particular pair was found to be indistinguishable by every combination of ratios (210 times or 100%). In addition, this pair was also found to be indistinguishable by μXRF, as referenced in Table 13, which concludes that these two fragments share very similar elemental profiles. There were 4 other indistinguishable pairs that were found by several of the ratio combinations, which were also found indistinguishable by LA-ICP-MS and/or μXRF, these pairs and the associated frequency of occurrence (out of a possible 210 combinations) are: 11:12 (28 times or 13.3%), 13:14 (7 times or 3.3%), 23:24 (84 times or 40.0%), and 28:29 (84 times or 40.0%). Actual sample descriptions for these pairs can be found in Table 13 where indistinguishable pairs by LIBS are depicted by the superscript “a”.

3.4.2.2 XRF

The XRF discrimination results concluded 14 indistinguishable pairs (98.3 % discrimination) using the three-sigma criteria discussed earlier. Again, this approach is routinely used in casework by the Florida Department of Law Enforcement (FDLE) and has been in place and validated through years of experience and multiple studies. Of these pairs, only three originated from different vehicles, each of these given pairs were discriminated by application of the t-test at the 95% confidence interval. Therefore, application of the t-test at the 95% confidence interval to the remaining 11 pairs yielded 8 indistinguishable pairs out of a possible 820 comparisons (the number of possible pairs is equal to N(N-1)/2, where N is the number of samples). This discrimination analysis

approach demonstrated 99.0% discrimination for XRF, which is excellent discrimination power.

Table 13. Description of the indistinguishable pairs found by LIBS, XRF, and LA-ICP-MS. [a] = indistinguishable pairs found by LIBS; [b] = indistinguishable pairs by XRF; [c] = indistinguishable pairs by LA-ICP-MS.

pair #	sample #	vehicle make	vehicle model	year	sample location
1[a,b]	6	Chevrolet	Cavalier	2004	outside windshield
	7	Chevrolet	Cavalier	2004	inside windshield
2[b,c]	8	Chevrolet	Cavalier	2004	side window
	9	Chevrolet	Cavalier	2004	rear window
3[a,b,c]	11	Oldsmobile	Intrigue	1998	outside windshield
	12	Oldsmobile	Intrigue	1998	inside windshield
4[a,b,c]	13	Dodge	Neon	2000	outside windshield
	14	Dodge	Neon	2000	inside windshield
5[b,c]	20	Chevrolet	Cavalier	2003	outside windshield
	21	Chevrolet	Cavalier	2003	inside windshield
6[a,b,c]	23	Dodge	Stratus	1998	outside windshield
	24	Dodge	Stratus	1998	inside windshield
7[a,b]	28	Ford	Expedition	2004	inside windshield
	29	Ford	Expedition	2004	outside windshield
8[b]	37	Jeep	Grand Cherokee	2001	outside windshield
	38	Jeep	Grand Cherokee	2001	inside windshield

Furthermore, all of the provided indistinguishable pairs have explanation as to why they exhibit similar elemental profiles. Each indistinguishable pair originated from the same vehicle and thus they have similar elemental profiles, meaning that the fragments (representing the glass source as a whole) were likely produced in the same manufacturing plant at about the same time period. Seven of the 8 pairs found indistinguishable were attributed to samples from the same laminated windshield (inside and outside fragments originating from the same windshield), while the eighth indistinguishable pair represents side and rear window fragments that also originated from the same vehicle. The pairs found indistinguishable overall by this method are listed and described in Table 13; in the given table the indistinguishable pairs found by XRF are labeled by the superscript “b”.

3.4.2.3 LA-ICP-MS

Pairwise comparison analysis (ANOVA with Tukey's post hoc test) yielded 11 indistinguishable pairs out of a possible 820 comparisons (or 98.7% discrimination). Six of these 11 pairs were discriminated by application of a t-test including three pairs that originated from different vehicles produced in different years. The end result is that these fragments should be discriminated and were by the combined discrimination analysis approach. Nevertheless, the other three pairs discriminated by t-test did originate from the same vehicle; the reason that some pairs were discriminated is likely due to a sampling and/or a precision-related issue. If the precision of the measurement for a given fragment is smaller than the overall precision of the glass pane as a whole, it is possible that fragments obtained from the same source (i.e. inside and outside fragments from the same windshield) can be discriminated. In forensic casework it is important that proper sampling techniques are followed to ensure that correct characterization of a glass source is achieved and that correct associations or discriminations are made.

The net result for LA-ICP-MS, combining ANOVA and t-test, was that five indistinguishable pairs were found out of a possible 820 pairs (equating to 99.4% discrimination). Remarkably, these five pairs were identical to five of the eight pairs found indistinguishable by XRF; therefore, despite LA-ICP-MS having slightly better discrimination power (0.4 % greater), the results are well correlated. The correlation between LA-ICP-MS and XRF data for this sample set will be addressed in the next section. The five indistinguishable pairs by LA-ICP-MS are summarized in Table 13 where the pairs marked with a superscript "c" represent the five indistinguishable pairs determined by LA-ICP-MS. The fact that both methods generated the same output, namely the same indistinguishable pairs, demonstrates the strength and validity of these two methods for forensic glass comparisons. Again, the indistinguishable pairs all had explanations as to why they exhibited very similar elemental profiles. The top discriminating elements by LA-ICP-MS and the associated results per element can be found in Table 14. Take note that the top discriminating element is strontium, which overall has been consistently a top discriminator for the trace elemental analysis of float glass. Therefore, given its wide variation across glass sample sets, including the one

studied in this research, strontium was the element chosen for the correlation studies in this work.

Table 14. Percent discrimination by element, LA-ICP-MS.

element	# indist. pairs	% discrimination
Sr	76	90.7
Zr	127	85.5
Ti	142	82.7
Rb	176	78.5
Ba	191	76.7
All (5)	5	99.4

3.4.3 Correlation Study

The three analytical techniques are compared in terms of concentration (LA-ICP-MS) versus intensity (XRF or LIBS), and the results are summarized here. Figure 14 shows the distribution of strontium (mean concentration or mean intensity), as determined by LIBS, XRF, and LA-ICP-MS. The plot shows the variation (or in some cases the association) of strontium in the glass sample set analyzed for this study; also, it partially demonstrates the correlation of the strontium signal for the three methods. It can be observed that when the strontium concentration or intensity is increased for one method (for instance, when going from one sample to the next), the strontium signal is also increased in similar magnitude for the other methods. Nevertheless, more descriptive correlations of such results can be found in Figure 15, where concentration (LA-ICP-MS) is plotted against intensity (XRF or LIBS) and the associated correlation coefficients are found.

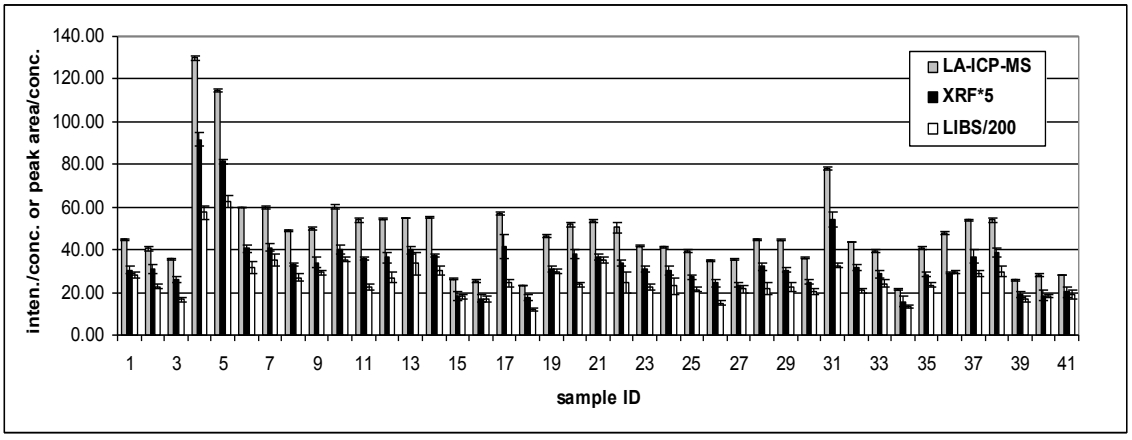

Figure 14. Strontium distribution among the 41 glass set, a comparison of means for XRF (signal intensity), LA-ICP-MS (concentration), and LIBS (peak area). Note that the LIBS intensities were divided by 200 and the XRF intensities were multiplied by 5.

The correlation between LA-ICP-MS and μXRF data using strontium mean concentrations and intensities (with the associated error bars), respectively, for the 41 glass set was plotted and compared. As depicted in Figure 15(a), a strong correlation between the two data sets is demonstrated, represented by a correlation coefficient of 0.9911. The excellent correlation between these two methods further establishes why similar discrimination results were obtained.

A correlation between LA-ICP-MS and LIBS data was also plotted using LA-ICP-MS strontium concentrations versus LIBS intensities for strontium (mean values with respective standard deviations) for the 41 glass set. As observed, the correlation for LIBS and LA-ICP-MS ($R^2 = 0.8813$) [reference Figure 15(b)] is not as strong as the correlation between the LA-ICP-MS and μXRF data sets ($R^2 = 0.9911$). However, the plot helps to illustrate the small degree of variation between sample replicates for LIBS using the setup outlined earlier (which is excellent for LIBS analyses) and by combining the observed precision with the correct choice of peak ratios provided excellent discrimination [60].

3.5 Conclusions

Discrimination of forensic glass fragments by LIBS exhibited humble beginnings as demonstrated by the early LIBS Crossfire results where discrimination power looked to be comparable (or actually worse) than what was reported in the literature by Bridge et al [38] ~53% discrimination versus ~83% discrimination, respectively. Nevertheless, a pursuit to achieve improvements soon followed; these improvements (and the resulting discrimination) were the product of both the method by which LIBS analyses were generated and the data analysis protocol that was developed to ensure accurate comparisons between sample fragments. The provided results regarding the most recent set of LIBS data was in part due to the tremendous help Dr. Cleon Barnett, who deserves his due credit in the evolution of forensic glass examinations by LIBS.

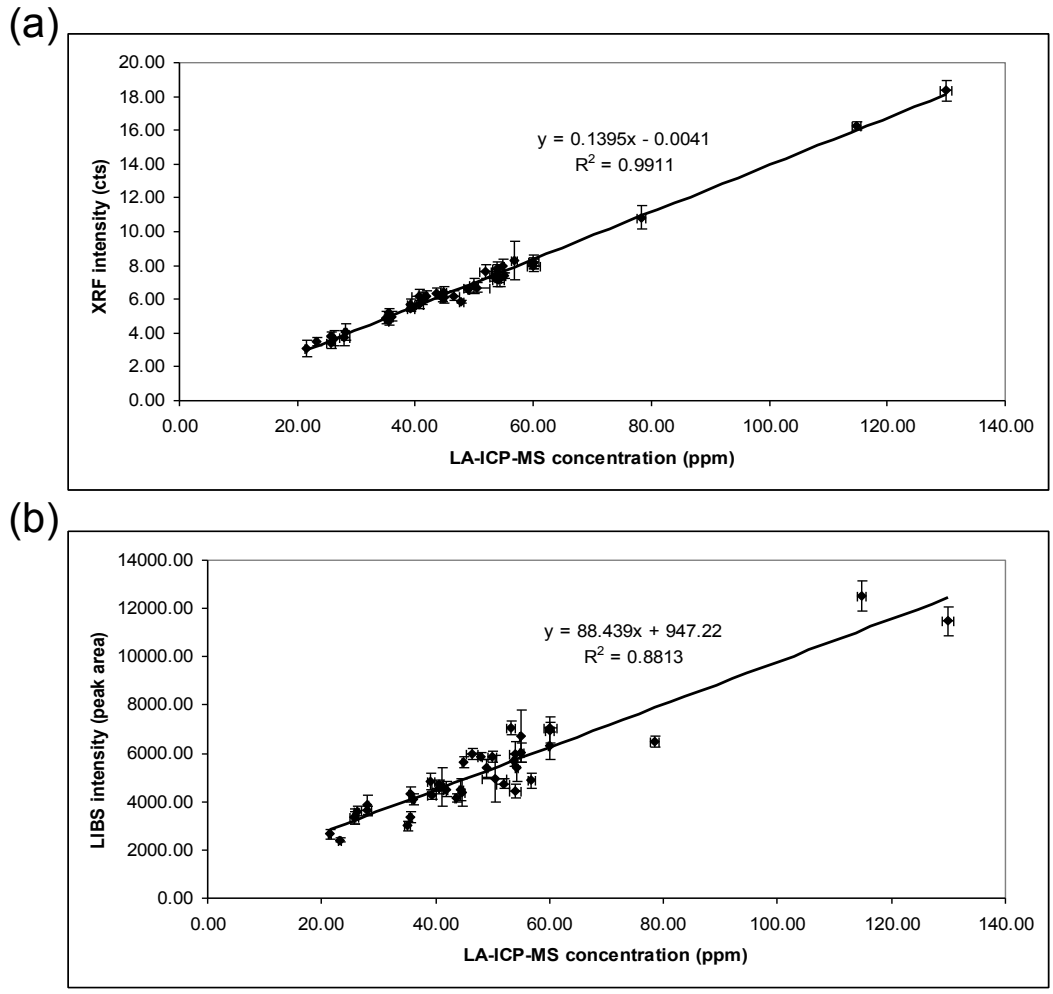

Figure 15. (a) Correlation of LA-ICP-MS and μXRF strontium results, (b) Correlation of LA-ICP-MS and LIBS strontium results; concentration versus peak area.

Nevertheless, two of the leading techniques in elemental analysis, LA-ICP-MS and XRF, were compared to a less mature technique, LIBS, in terms of discrimination power for a set of automotive glass samples. Significantly, all three analytical approaches yielded similar discrimination results (≥99% discrimination). Moreover, the five indistinguishable pairs found by LA-ICP-MS were the same as five of the eight indistinguishable pairs determined by XRF and many of the ratio combinations used to discriminate the glass samples by LIBS concluded the same pairs found indistinguishable by the other methods [60].

In addition, the indistinguishable pairs obtained for LA-ICP-MS, XRF and LIBS retained good explanation as to why the associated elemental profiles were similar and

thus could not be discriminated. These indistinguishable pairs originated from the same vehicle and thus were likely to have been manufactured in the same plant at about approximately the same time.

With respect to analyzing LIBS spectra and making sample comparisons, an extensive study was conducted comparing different data reduction procedures to ensure accurate discrimination. The probability of committing Type I or Type II errors was reduced and/or eliminated using the sample comparison approach outlined in the paper; reducing these types of errors is especially crucial for forensic casework. The net result was a data reduction protocol being adopted and then utilized to successfully discriminate the glass sample set of interest. The best combination of ratios produced only 1 indistinguishable pair (out of the possible 820 pairs) and this pair was explainable.

Furthermore, 10 ratios are suggested are thus considered optimum for the analysis and discrimination of glass by LIBS based the data analysis study outlined. Those proposed ratios include: 394.4nm/330.0nm (Al/Na), 766.5nm/643.9nm (K/Ca), 394.4nm/371.9nm (Al/Fe), 438.4nm/766.5nm (Fe/K), 534nm/766.5nm (Ca/K), 371.9nm/396.2nm (Fe/Al), 766.5nm/645.0nm (K/Ca), 394.4nm/460.7nm (Al/Sr), 460.7nm/766.5nm (Sr/K), and 818.3nm/766.5nm (Na/K).

In summation, given its low cost, high sample throughput, good sensitivity, and ease of use, the application of LIBS for forensic glass examinations looks promising and can present a viable alternative to LA-ICP-MS and XRF in the forensic laboratory.

4. IMPROVEMENTS IN THE STANDARDIZATION OF LIBS FOR FORENSIC ANALYSIS OF GLASS

This last chapter is devoted to reporting the results from the continuation of the original award and the emphasis of this continuation was to developed a more standardized method for LIBS analysis of glass. A second aim was to better engage the instrument manufacturers in order to better guide the companies that were interested in commercializing LIBS instrument to pay attention to the forensic applications possible. In order for LIBS to be adopted into the forensic laboratory, instrument manufacturers have to design, build and market suitable instrumentation for the forensic laboratory. Foster and Freeman was the first company to enter this market and was soon followed by Ocean Optics, Photon Machines, Applied Spectra and Applied Photonics. Our efforts

have incorporated 4 of the 5 instrument manufacturers in order to provide feedback for some fundamental issues of interest to forensic scientists.

4.1 Irradiation wavelength selection

The first parameter that is important to consider in LIBS standardization and instrument optimization is the irradiation wavelength. As previously discussed in chapter 3 of this report, the LIBS system used was a custom-built system that could be configured for 266 nm, 532 nm or 1064 nm irradiation. One publication from the effort reports the advantages of 266 nm in terms of damage to the surface of small glass fragments [61] while a second publication reports the advantages in precision for 266 nm vs 1064 nm [58]. Figures 16 and 17 below illustrate the differences between 266 nm irradiation (figure 16 top) and 1064 nm irradiation (figure 16 bottom).

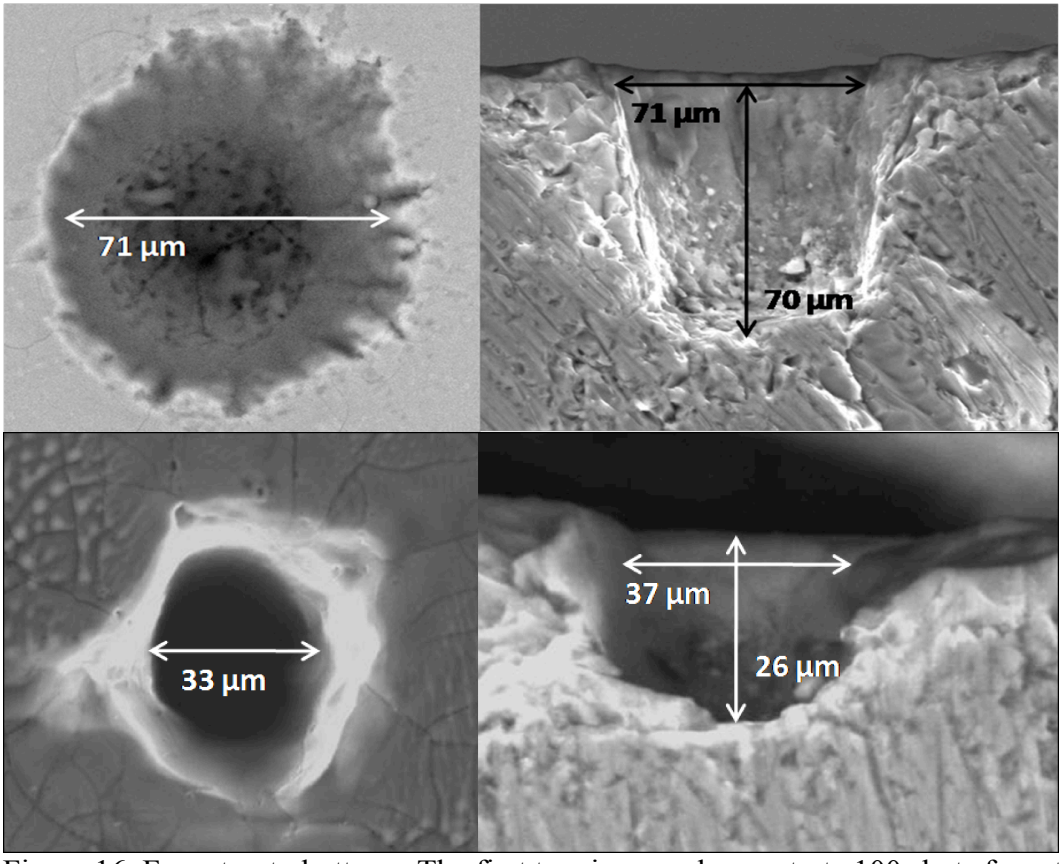

Figure 16. From top to bottom: The first two images demonstrate 100 shots from the UV, 266 nm laser. Total mass removal is approximately 790 ng. This value is relatively constant for all SP configurations. The second two images demonstrate 100 shots from the IR, 1064 nm laser. Total mass removal is approximately 81 ng.

It should be noted that in Figure 16, there is more mass removed from the 266 nm irradiation, primarily due from the improved coupling between the UV laser vs the IR laser.

More importnatly, when the power was not optimized, as in the case of Figure 17, the craters resulting from 1064 nm irradiation led to large cracking and even breaking apart of glass samples. This observation was very typical when the commercial instruments were used as these instruments did not provide fine control of irradiation energy and therefore the typical crater morphology resembled the crater found in figure 17. This lack of uniformity in morphology also translated to less precise data in the analysis [58].

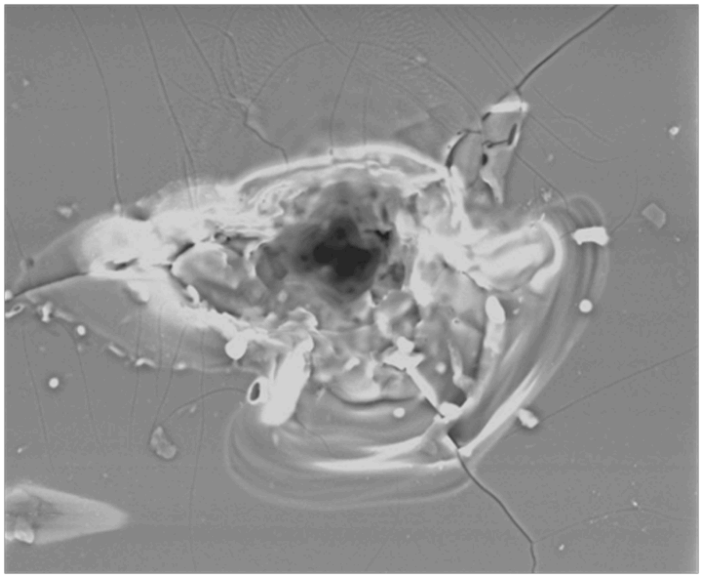

Figure 17. Damage of glass by cracking and irregular crater shapes occur by too high of IR laser power. The IR irradiance does not couple well into glass material.

The calibration plots in Figure 18 and the data in Table 15 below also illustrate the improvement in precision for the 266 nm irradiation vs 1064 nm irradiation. This trend was also observed for 532 nm irradiation [61] although not as pronounced as for the 1064 nm, both vs the 266 nm irradiation. One conclusion and subsequent recommendation for instrument manufacturers is that the better coupling from 266 nm irradiation does translate into better precision data and therefore better discrimination. One major disadvantage to the 266 nm laser is that it is typically 40-50% more expensive than the same energy 1064 nm laser. Instrument manufacturers are thus hesitant to incorporate the more expensive laser into commercial systems and our efforts have been devoted to better inform users and manufacturers of these results.

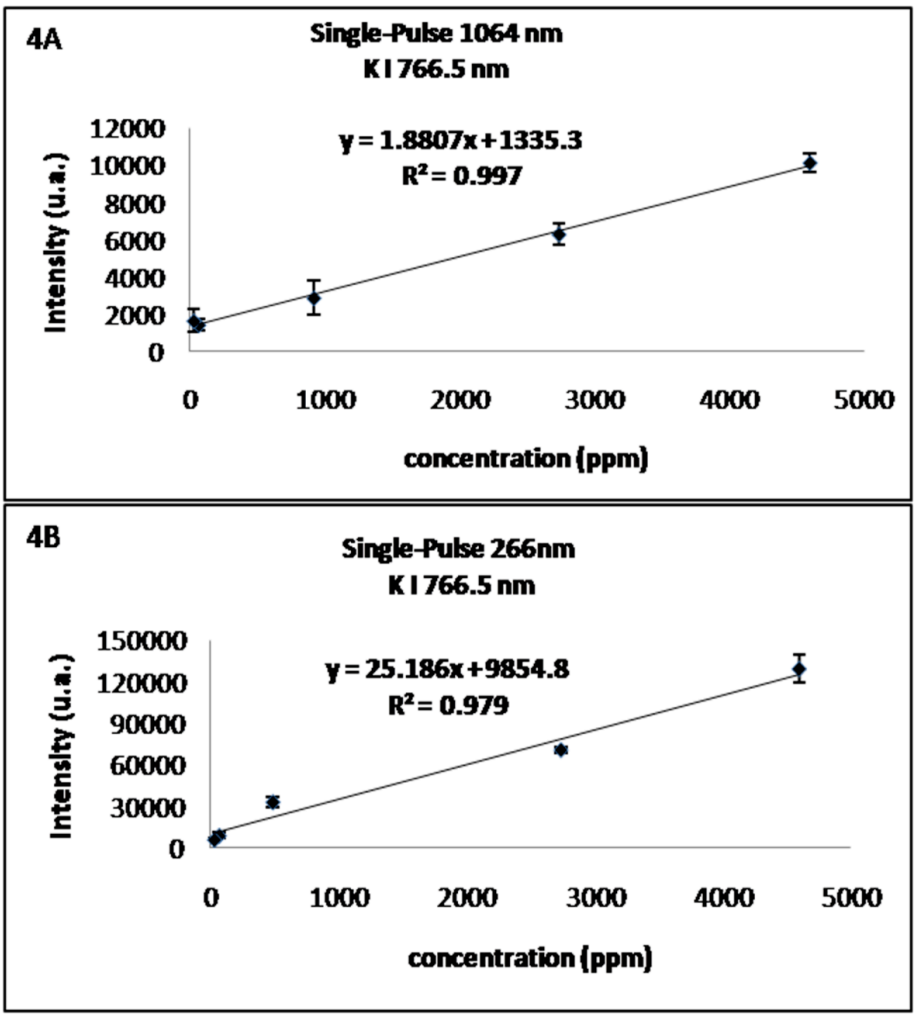

Figure 18. Comparison of precision for 266 nm (bottom) and 1064 nm (top) irradiation for glass analysis by LIBS. The error bars for the 266 nm irradiation were improved over 1064 nm.

Table 15. Comparison between single pulse (SP) 266 nm (UV) irradiation and SP 1064 nm irradiation (IR) in terms of precision and accuracy.

Method	Sample	Peak	Precision (%)	Bias (%)
SP UV	1831	K I 766 nm	**8.23**	**12.15**
SP UV	1831	Ba II 493 nm	**10.83**	**8.18**
SP IR	1831	K I 766 nm	30.00	38.23
SP IR	1831	Sr II 421 nm	14.88	18.37

Even with less uniform crater shape, IR is still able to produce reliable data. The more efficient ablation however translates to better precision. Please take not of the error bars on the calibration curves, the UV precision is better than the precision on the IR. With

the more efficient ablation and increased precision, 266 nm is the choice wavelength for the forensic analysis of glass.

4.2 Atmosphere above the sample

Argon gas serves as an insulator and as a plasma conductor. When performing LIBS in an argon atmosphere, the argon environment increases the plasma temperature and the plasma lifetime which renders more complete ionization. The LIBS signal is therefore enhanced. Figure 19 illustrates the Sr II 407 peak when the 1831 NIST glass standard is analyzed and the concentration of the Sr in this standard is reported to be 89 ug/g (ppm). The smaller peak in the figure is observed when the experiment is conducted in air and without an argon environment and the more intense peak is formed while flooding the sample surface with a flow of Ar at 900 mL/min. There is then a 3 times increase in the signal-to-noise ratio from 32 to 99 for the LIBS experiment under Ar atmosphere. These results were communicated to the instrument manufacturers and they all now include the option of introducing Ar gas into the sample chamber for the analysis.

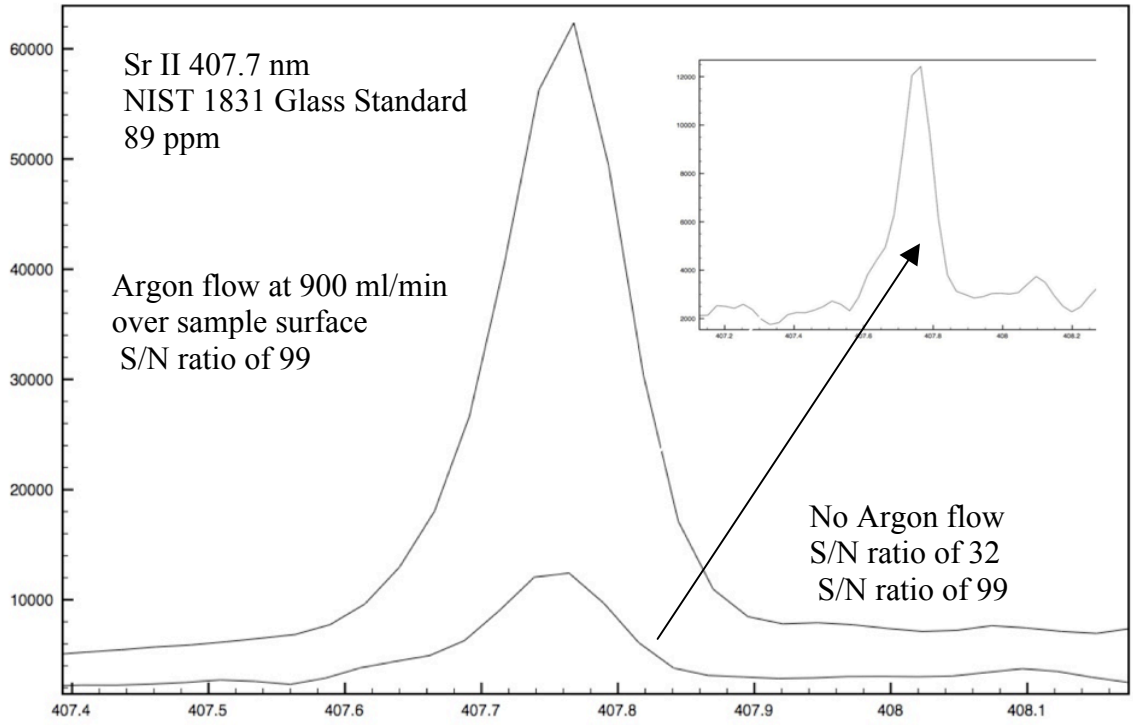

Figure 19. Differences in signal-to-noise ratio for the LIBS analysis of NIST 1831 glass standard with and without Ar introduction into the sample chamber.

In addition, the measurement precision and accuracy were also evaluated when Ar was added above the sample and, indeed, an improvement in precision, bias as well as detection limits were observed for these determinations. Table 16 below summarizes the improved precision, bias a limits of detection for the Ar experiment when all the other variables were held constant. The instrumental setup for this experiment is found in figure 20.

Table 16. Comparison of precision, bias and limits of detection for the analysis of NIST 1831 glass standard with and without an Argon atmosphere above the sample.

Method	Sample	Peak (nm)	Precision (%)	Bias (%)	LOD (ppm)	LOQ (ppm)
SP UV	1831	Sr II 407.7	5.8	9.5	4.10	13.68
SP UV	1831	Ba II 493.4	10.8	9.5	2.25	7.51
SP UV	1831	K I 766.5	8.2	12.2	5.93	19.77
SP UV Ar	1831	Sr II 407.7	4.5	7.3	1.08	3.59
SP UV Ar	1831	Ba II 493.4	4.6	1.04	1.1	3.66
SP UV Ar	1831	K I 766.5	1.6	2.64	3.93	13.10

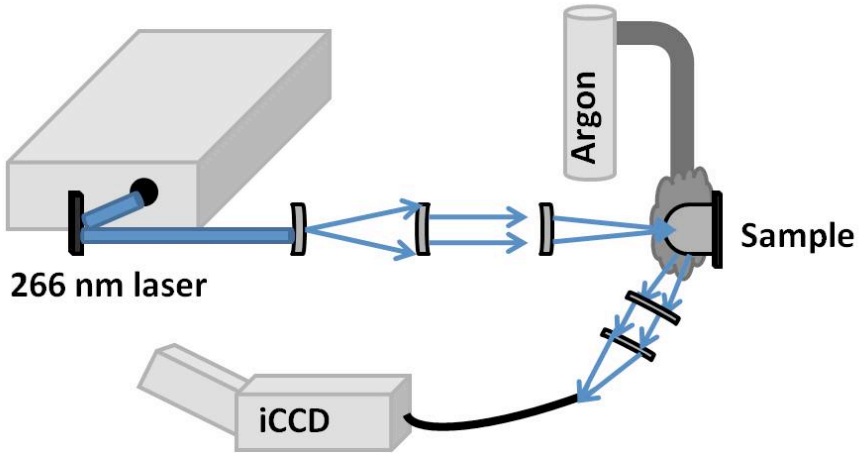

Figure 20. Experimental and instrumental setup for the Ar experiment using a single pulse 266 nm laser (29 mJ), and Andor Mechelle spectrometer coupled to an Andor istar ICCD camera. The gate delay was 1.5 μs and the gate width was 12.0 μs. The laser was focused into the sample 1.30 mm and the spectra obtained (Table 1) was an accumulation of 50 laser shots.

The collaboration with the Winefordner group also confirmed our results that focusing the laser into the sample ~ 1 mm produced more intense spectra that were more precise

and accurate [62-63]. These results should be taken into account in the development of a "standard method" for LIBS analysis.

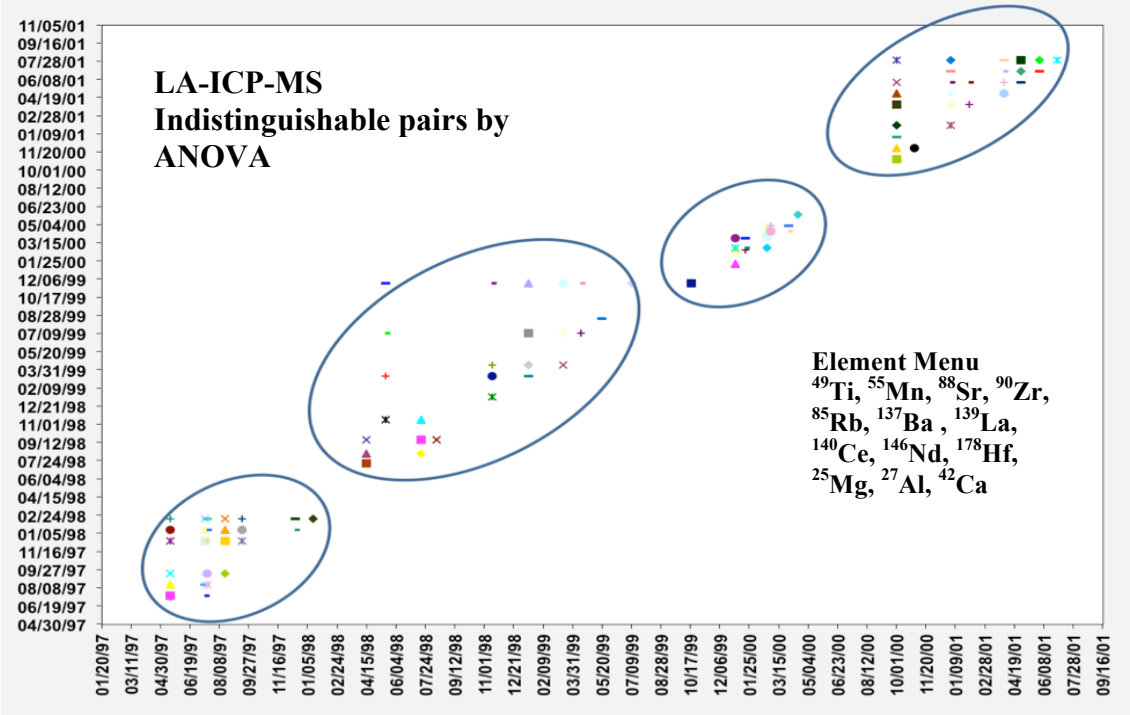

Figure 21. Points indicating the indistinguishable pairs resulting from a pairwise comparison of LA-ICP-MS data from glass manufatured on one date (y axis) with glass manufactured on another date (x-axis) in the same manufacturing plant.

Finally, the LIBS technique was compared in discrimination performance to the more mature LA-ICP-MS method for discrimination of glass. Figure 21 above represents data resulting from the LA-ICP-MS analysis of glass from a float glass manufacturer in Portage, Wisconsin (Cardinal Glass Industries). Forty nine (49) samples were analyzed, these samples we taken from 1997 to 2001 with some only being two weeks apart. All of these sample, spanning ~ 4 years of production are not distinguishable by RI due to the very narrow range of RI values. The figure illustrates that glass production can be indistinguishable up to several weeks apart from the manufacturing date but when samples are manufactured months or years apart, the samples can be distinguished by comparing the element menu listed in the figure (also see Chapters 2 and 3 above).

The circles in this figure represent glass samples that are similar in elemental composition. The top three elements here were determined to provide the most discrimination. This figure demonstrates the chemical composition of glass can easily be

distinguished by LA ICP MS over a time frame usually greater than two weeks. The indistinguishable pairs are those manufactured close in time. These results are reported in a publication that is in preparation [57].

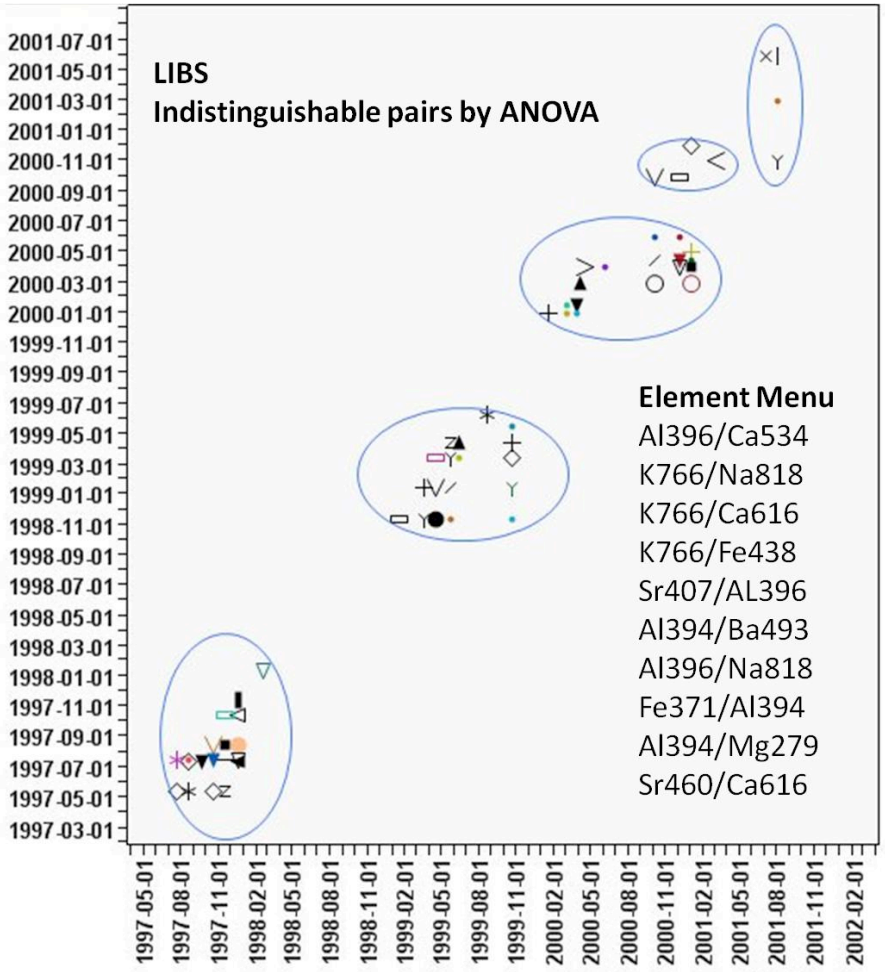

Figure 22. Points indicating the indistinguishable pairs resulting from a pairwise comparison of LIBS data from glass manufatured on one date (y axis) with glass manufactured on another date (x-axis) in the same manufacturing plant.

As part of this study, the same samples of float glass were then analyzed by LIBS. This plot represents the indistinguishable pairs determined by ANOVA using LIBS. As demonstrated here, LIBS provides very similar results as compared to LA-ICP-MS, even able to discriminate samples manufactured in the same glass plant. The discrimination power is approximately the same as LA-ICP-MS. One can see from figure 22, again, that the indistinguishable pairs that are manufactured very close in time, generally two to three weeks apart are found to be indistinguishable by LIBS but when glass is manufactured more than ~ 2 weeks apart, these can generally be distinguished.

5. CONCLUSIONS

The work presented in this report has outlined results that will certainly help the forensic community with respect to glass. In the first part of the research, nanosecond LA-ICP-MS was proven to offer similar figures of merit for the forensic analysis of glass (in terms of accuracy, precision and discrimination power) when compared to femtosecond LA-ICP-MS, which was hypothetically expected to outperform nanosecond LA-ICP-MS. It was also shown that an internal standard was necessary in order to obtain accurate and precise results for both methods, meaning that internal and matrix matched standardization are important to ensure optimum quantitative analyses by LA-ICP-MS, whether the laser be a nanosecond source or a femtosecond source. The observed comparable results by nanosecond and femtosecond LA-ICP-MS is attributed to the utilization of quantification from a glass matrix-matched standard, which is readily available to the forensic scientific community. In cases where a matrix-matched standard is not available (and in some cases a good internal standard is not available), femtosecond LA-ICP-MS could provide improved results (in terms of precision and discrimination potential) over nanosecond LA-ICP-MS analyses for the same matrix.

Laser induced breakdown spectroscopy (LIBS) was introduced for the analysis of glass, which was shown to provide similar discrimination potential (>99% discrimination) for an automotive glass sample set of forensic interest when compared to two of the leading techniques in elemental analysis, uXRF and LA-ICP-MS. A strict protocol for data evaluation of LIBS spectra was evaluated and then followed to minimize Type I (false exclusion) errors and eliminate Type II (false inclusion) errors, which ultimately addresses the concerns outlined by the National Research Council's report on forensic analyses. Overall, a method using LIBS has been developed, optimized, and validated for the forensic analysis of float glass, which due to its low cost, reduced complexity (user friendliness), faster analysis time, and capability of being a portable technique, makes LIBS a viable alternative to XRF and LA-ICP-MS for the elemental analysis of glass.

6. REFERENCES

[1] Hickman D (1986) Forens Sci Intern 33:23-46

[2] Ryland S (1986) J Forens Sci 31:1314

[3] Almirall JR, Trejos T (2007) Forensic Sci Rev 18:73-96

[4] Maloney FJT (1968) Glass in the Modern World Doubleday: New York, NY

[5] Almirall JR (2001) Elemental Analysis of Glass Fragments. In: Caddy B (Ed) Trace Evidence Analysis and Interpretation: Glass and Paint. Taylor and Francis, London

[6] Buscaglia J (1994) Anal Chim Acta 288:17-24

[7] Almirall JR (2001) Glass as Evidence of Association In: Houck M (Ed) Mute Witness When Trace Evidence Makes the Case. Academic Press, San Diego, CA

[8] ASTM Annual Book of ASTM Standards (2004) American Society for Testing and Materials 14.02, 1

[9] Trejos T, Montero S, Almirall JR (2003) Anal Bioanal Chem 76:1255-1264

[10] Trejos T, Almirall JR (2004) J Anal Chem 76:1236-1242

[11] Trejos T, Almirall JR (2005) Talanta 67:388-395

[12] Trejos T, Almirall JR (2005) Talanta 67:396-401

[13] Latkoczy C, Ducking M, Becker S, Gunther D, Hoogewerff J, Almirall JR, Buscaglia J, Dobney A, Koons R, Montero S, van der Peijl GJQ, Stoechlein W, Trejos T, Watling RJ, Zdanowicz V (2005) J Forensic Sci 50:1327-1341

[14] Russo RE, Mao X, Liu H, Gonzalez J, Mao SS (2002) Talanta 57:425-451

[15] Gunther D, Hattendorf B, Latkoczy C (2003) Anal Chem 341A-347A

[16] Russo RE, Mao X, Mao SS (2002) Anal Chem 74:70A-77A

[17] Gonzalez J, Liu C, Wen S, Mao X, Russo RE (2007) Talanta 73:567-576

[18] Gonzalez J, Liu C, Wen S, Mao X, Russo RE (2007) Talanta 73:577-582

[19] Koch J, von Bohlen A, Hergenroder R, Niemax K (2004) J Anal At Spectrom 19:267-272

[20] Russo RE, Mao X, Gonzalez JJ, Mao SS (2002) J Anal At Spectrom 17:1072-1075

[21] Gonzalez J, Lui CY, Mao XL, Russo RE (2004) J Anal At Spectrom 19:1165-1168

[22] Russo RE, Mao X, Gonzalez JJ, Mao SS (2002) J Anal At Spectrom 17:1072-1075

[23] Poitrasson F, Mao X, Mao S, Freydier R, Russo RE (2003) Anal Chem 75:6184-6190

[24] Gonzalez J, Dundas SV, Lui CY, Mao X, Russo RE (2006) J Anal At Spectrom 21:778-784

[25] Montaser A (1998) Inductively Coupled Plasma Mass Spectrometry, Wiley-VCH, New York

[26] Skoog DA, Holler FJ, Nieman TA (1998) Principles of Instrumental Analysis, 5th Edition, Harcourt Brace, PA

[27] Denoyer ER, Tanner SD, Voelkopf U (1999) Spectroscopy 14:43

[28] Tanner SD, Baranov VI (1999) J Anal At Spectrom 10:1083

[29] Hattendorf B, Gunther D (2000) J Anal At Spectrom 15:1125

[30] Rowan JT, Houk RS (1989) Appl Specrosc 43:976

[31] Beauchemin D (2002) Anal Chem 74:2873

[32] Trahey N (Ed) (1998) NIST Standard Reference Material Catalog 1998-1999, National Institute of Standards and Technology

[33] Longerich HP, Jackson SE, Gunther D (1996) J Anal At Spectrom 11:899-904

[34] Guillong M, Gunther D (2002) J Anal At Spectrom 17:831-837

[35] Lui C, Mao XL, Mao SS, Greif R, Russo RE (2004) Anal Chem 76:379-383

[36] Naes B, Umpierrez S, Ryland S, Barnett C, Almirall JR (2008) Spectrochim Acta B

[37] Rodriquez-Celis EM, Gornushkin IB, Heitmann UM, Almirall JR, Smith BW, Winefordner JD, Omenetto N (2008) 391:1961-1968

[38] Bridge CM, Powell J, Steele KL, Williams M, MacInnis JM, Sigman ME (2006) Applied Spectrosc 60:1181-1187

[39] Scaffidi J, Angel SM, Cremers DA (2006) Anal Chem A-pages (Jan.1)

[40] Vadillo JM, Laserna JJ (2004) Spectrochim Acta B 59:147-161

[41] Brunelle RL, Crawford KR (2002) Advances in the Forensic Analysis and Dating of Writing Ink, Charles C Thomas Publisher, Springfield, IL

[42] Anglos D (2001) Applied Spectrosc 55:186-205A

[43] Maind SD, Kumar SA, Chattopadhyay N, Gandhi C, Sudersan M (2005) Forensic Sci Intern 159:32-42

[44] Zieba-Palus J, Kunicki M (2005) 158:164-172

[45] Fittschen UE, Bings NH, Hauschild S, Forster S, Kiera AF, Karavani E, Fromsdorf A, Thiele J (2008) Anal Chem 80:1967-1977

[46] Spence LD, Baker AT, Byrne JP (2000) J Anal At Spectrom 15:813-819

[47] Koons R, Fiedler C, Rawalt R (1998) J Foren Sci 33:49-67

[48] Becker S, Gunaratnam L, Hicks T, Stoecklein W, Warman G (2001) Prob of Forens Sci XLVII:80-92

[49] Gamaly EG, Rode AV, Luther-Davies B (1999) J Appl Phys 85:4213

[50] Rode AV, Luther-Davies BE, Gamaly G (1999) J Appl Phys 85:4222

[51] Mao S, Mao XL, Greif R, Russo RE (2000) Appl Phys Lett 77:2464

[52] Mao SS, Mao XL, Greif R, Russo RE (2000) Appl Phys Lett 76:3370

[53] Mao XL, Russo RE (1996) Appl. Phys. A: Mater. Sci. Process 64:1

[54] Liu HC, Mao XL, Yoo JH, Russ RE (1999) Spectrochim Acta Part B 54:1607

[55] Phipps CR, Dreyfus RW (1993) In Laser Ionization Mass Analysis Vertes RG, Adams F (Ed) Wiley: NY

[56] E Cahoon, C Barnett and JR Almirall, , *Applied Spectroscopy; Focal Point Paper*, in preparation.

[57] EM Cahoon and JR Almirall, *Analytical and Bioanalytical Chem.,* in preparation.

[58] EM Cahoon and JR Almirall, *Applied Optics*, 2010, 49(13), C49-C57.

[59] W Castro, T Trejos, B Naes and JR Almirall, *Analytical and Bioanalytical Chem*, 2008, 392 (4), 663-672.

[60] B Naes, S Umpierrez, S Ryland, C Barnett and JR Almirall, *Spectro Acta B: Atom Spec*, 2008, 63 (10), 1145-1150.

[61] C Barnett, E Cahoon and JR Almirall, *Spectrochimica Acta Part B: Atomic Spectroscopy* 2008, 63 (10), 1016-1023.

[62] EM Rodriguez-Celis, IB Gornushkin, JR Almirall, N Omenetto, BW Smith, JD Winefordner, *Analytical and Bioanalytical Chemistry*, 2008, 391(5), 1961-1968.

[63] JR Almirall, S Umpierrez, W Castro, I Gornushkin and J Winefordner, *Sensors, and Command, Control, Communications, and Intelligence Technologies for Homeland Defense and Law Enforcement*, E.M. Carapezza, Ed., Proceedings of the SPIE - The International Society for Optical Engineering, 2005, 5778, 657-666.

7. Dissemination of Research Findings.

The following appendices (A, B and C) list the number of scientific peer-reviewed publications (Appendix A) and presentations (Appendix B) that were derived from this work. Publications 1 and 2 are in preparation and are expected to be submitted to a journal by Dec. 1, 2010. A total of 8 scientific publications and a total of 45 scientific presentations were derived from this effort. A copy of each of the publications (3-7) are included as an attachment in Appendix C.

Appendix A – Peer-reviewed **publications** derived from this work.

1. E Cahoon, C Barnett and **JR Almirall,** Laser Induced Breakdown Spectroscopy (LIBS) in Forensic Analysis, *Applied Spectroscopy; Focal Point Paper*, in preparation.

2. EM Cahoon and **JR Almirall,** Discrimination and Association of Glass Fragments using a Standardized LIBS Method, *Analytical and Bioanalytical Chem.,* in preparation.

3. EM Cahoon and **JR Almirall,** Wavelength Dependence on the Forensic Analysis of Glass by Laser Induced Breakdown Spectroscopy, *Applied Optics*, **2010**, 49(13), C49-C57.

4. W Castro, T Trejos, B Naes and **JR Almirall**, Comparison of the Analytical Capabilities of High Resolution Sector Field Inductively Coupled Plasma Mass Spectrometry and Dynamic Reaction Cell Inductively Coupled Plasma Mass Spectrometry for the Forensic Analysis of Iron in Glass Samples, *Analytical and Bioanalytical Chem*, **2008**, 392 (4), 663-672.

5. B Naes, S Umpierrez, S Ryland, C Barnett and **JR Almirall**; A Comparison of Laser Ablation Inductively Coupled Plasma Mass Spectrometry (LA-ICP-MS), Micro X-Ray Fluorescence (μXRF), and Laser Induced Breakdown Spectroscopy (LIBS) for the Discrimination of Automotive Glass, *Spectro Acta B: Atom Spec*, **2008**, 63 (10), 1145-1150.

6. C Barnett, E Cahoon and **JR Almirall**, Wavelength Dependence on the Elemental Analysis of Glass by LIBS, *Spectrochimica Acta Part B: Atomic Spectroscopy* **2008**, 63 (10), 1016-1023.

7. EM Rodriguez-Celis, IB Gornushkin, JR Almirall, N Omenetto, BW Smith, **JD Winefordner**, Laser Induced Breakdown Spectroscopy as a Tool for Discrimination of Glass for Forensic Applications, *Analytical and Bioanalytical Chemistry*, **2008,** 391(5), 1961-1968.

8. JR Almirall, S Umpierrez, W Castro, I Gornushkin and J Winefordner, Forensic Elemental Analysis of Materials by Laser Induced Breakdown Spectroscopy (LIBS), in

Sensors, and Command, Control, Communications, and Intelligence Technologies for Homeland Defense and Law Enforcement, E.M. Carapezza, Ed., Proceedings of the SPIE - The International Society for Optical Engineering, **2005**, 5778, 657-666.

Appendix B – Peer-reviewed **presentations** derived from this work.

1. October 2010. Laser-based micro-spectrochemical analysis of materials in forensic examinations, University of South Carolina, Department of Chemistry and Biochemistry Seminar, Columbia, SC (**PA, Invited Oral)**

2. September 2010. LIBS Strategies for Quantitative Analysis, International LIBS 2010 Meeting, Memphis, TN (**PA, Invited Oral**)

3. September 2010. Characterization of materials by elemental analysis; μXRF, LA-ICP-MS and LIBS methods, match criteria and significance of association, Australian and New Zealand Forensic Science Society (ANZFSS) Meeting, Sydney, Australia **(PA, Oral)**

4. August 2010. Analysis of glass samples from a single manufacturing plant, NIJ Sponsored Elemental Analysis Working Group Breckenridge, CO **(Oral, SP)**

5. May 2010. Elemental Analysis of Float Glass comparing LA-ICP-MS, μXRF and LIBS, American Chemical Society FAME (Florida Annual Meeting and Exposition) Palm Harbor, FL (**PA, Invited Oral and Session Organizer**)

6. May 2010. Elemental Analysis of Float Glass by Working Groups comparing LA-ICP-MS, μXRF and LIBS, FAME Meeting, Palm Harbor, FL (**SP, Oral**)

7. February 2010, Towards a Standardized Chemical Characterization of Glass by Laser Induced Breakdown Spectroscopy (LIBS), AAFS Conference, Seattle, WA (**SP, Oral**)

8. February 2010, Analytical LIBS in Forensic Applications, Lawrence Berkeley National Laboratory, Berkeley, CA (**PA, Invited Oral**)

9. January 2010, Forensic Applications of Laser Induced Breakdown Spectroscopy, Department of Chemistry, University of East Anglia, Norwich, UK (**PA, Invited oral**)

10. January 2010, Advances in the Forensic Application of Laser Induced Breakdown Spectroscopy, Winter Conference on Plasma Spectrochemistry, Naples, FL (**PA, Invited Oral)**

11. July 2009, Wavelength Dependance on the Forensic Analysis of Glass by LIBS, North American Symposium on LIBS, New Orleans (**SP, Poster, Best Research Group Presentations**)

12. July 2009, Forensic Analysis of Container Glass by Laser Induced Breakdown Spectroscopy (LIBS), NASLIBS 2009, New Orleans (**SP, Poster, Best Research Group**)

13. July 2009, Forensic Science Applications of Laser Induced Breakdown Spectroscopy, NASLIBS 2009, New Orleans, (**PA, Invited Oral**)

14. May 2009, Shadowgraphy to Monitor Laser Induced Breakdown Spectroscopy (LIBS) Optimization Parameters for the Analysis of Glass Samples, FAME 2009, Orlando, FL (SP)

15. March 2009, Laser Induced Breakdown Spectroscopy (LIBS) for Surface Characterization: Chemical Mapping of Deposited Material, American Chemical Society, Salt Lake City, UT (SP)

16. September 2008, Quantitative LIBS analysis of sub-nanogram amounts of metals delivered on surfaces, International LIBS 2008 Conference, Berlin, Germany **(PA, Oral)**

17. April 2008, Plasma Shadowgraphy as a Diagnostic for Laser Induced Breakdown Spectroscopy to Optimize the Focusing Parameters for the Analysis of Glass Samples, American Chemical Society Meeting, New Orleans LA (**SP, Poster**)

18. April 2008, Project Updates; LIBS and SPME-IMS Research Progress, Technical Working Group on General Forensics-NIJ, Washington D.C., (**PA, Invited Oral**)

19. March 2008, The Analysis of Glass by Laser Ablation Inductively Coupled Plasma Mass Spectrometry, a Comparison of Nanosecond Laser Ablation to Femtosecond Laser Ablation, Pittsburgh Conference, New Orleans LA (**SP, Poster**)

20. March 2008, Forensic Elemental Analysis of Materials Using LIBS, u-XRF and LA-ICP-MS, Pittsburgh Conference, New Orleans, LA (**Invited Keynote, Oral**)

21. February 2008, Laser Induced Breakdown Spectroscopy (LIBS) and X-Ray Fluorescence (XRF) Analyses of Biological Matrices, AAFS, Washington D.C. (**SP, Poster**)

22. January 2008, Effects of Wavelength on LIBS of Glass and Metal Oxides Pellets, Environmental and Biological Applications of Laser (EBAL), Cairo, Egypt. (**SP, Oral**)

23. January 2008, Status of Plasma Spectrochemical Analysis in Forensic Science, Winter Plasma Conference, San Diego, CA (**Invited Keynote, with T. Trejos**)

24. October 2007, Forensic Applications of Laser Induced Breakdown Spectroscopy, Federation of Analytical Chemistry and Spectroscopy Societies, Memphis, TN (**PA**)

25. October 2007, Effects of Wavelength and Dual Pulse LIBS Schemes on Metal Oxides in Pellets, NASLIBS, New Orleans, LA, **(SP)**

26. October 2007, Chemical Characterization of Forensic Samples Using LIBS, NASLIBS, New Orleans, LA, **(PA)**

27. September 2007, Analytical LIBS of Forensic Samples, EMSLIBS, Paris, France **(PA)**

28. September 2007, Wavelength Dependence of LIBS analysis on Glass, EMSLIBS, Paris, France (**SP**)

29. August 2007, Interpretation of Data from the Forensic Analysis of Glass, Virginia Department of Forensic Sciences, Richmond, VA (**Invited Speaker, PA**)

30. August 2007, New Developments in Elemental Analysis of Glass Evidence, Trace Evidence Symposium (NIJ-FBI), St. Petersburg, FL, (**Invited Speaker, PA**)
31. August 2007, Elemental Analysis Workshop, Trace Evidence Symposium, St. Petersburg, FL, (**Instructor, PA**)

32. July 2007, Glass Examination and Comparison Workshop, Johnson County Sheriff's Office, Kansas City, KS (**Instructor, PA**)

33. July 2007, Glass Examination and Comparison Workshop, California Criminalistics Institute, Sacramento, CA (**Instructor, PA**)

34. Feb. 2007, New Developments in Forensic Applications of Laser Induced Breakdown Spectroscopy (LIBS), The Pittsburgh Conference, Chicago, IL (**PA**, **Invited Speaker**)

35. Feb. 2007, New Developments in Forensic Applications of Laser Ablation-ICP-MS, The Pittsburgh Conference, Chicago, IL (**PA**, **Invited Speaker**)

36. Feb. 2007, Forensic Analysis of Glass by LIBS, a Comparison to XRF and LA-ICP-MS for Elemental Profiling, AAFS Meeting, San Antonio, TX (SP, Oral)

37. Feb. 2007, Micro-homogeneity studies of trace elements in solid matrices by LA-ICP-MS: Implications for forensic comparisons, AAFS Meeting, San Antonio, TX (SP, Oral)

38. Feb. 2007, Comparison of Femtosecond (fs) vs Nanosecond (ns) Laser Ablation Sampling Coupled to ICP-MS for the Analysis of Glass and Other Matrices of Interest to Forensic Scientists, AAFS Meeting, San Antonio, TX (SP, Poster)

39. September 2006, "A Novel LIBS system for Forensic Analysis of Materials", FACSS, Orlando, FL. **(PA and Session Organizer)**

40. September 2006, "Forensic Glass Identification by Laser Induced Breakdown Spectroscopy", FACSS, Orlando, FL. (SP, Poster with Mariela Rodriguez, U. of Florida)

41. September 2006, "Forensic Elemental Analysis of Glass by LIBS, XRF and LA-ICP-MS", LIBS 2006 Conference, Montreal, Canada **(PA)**

42. September 2006, "Discrimination of Forensic Glass Fragments by Laser Induced Breakdown Spectroscopy, LIBS 2006 Conference, Montreal, Canada (SP)

43. February-March 2006, "Glass as a Model Matrix for LA-ICP-MS and LIBS", in ***Elemental Analysis of Forensic Evidence Workshop,*** FIU/NIJ Workshop, Chemistry and Biochemistry, Florida International University, Miami, FL **(Workshop Organizer, PA)**

44. Feb. 2006, Forensic Elemental Analysis of Glass by Laser Induced Breakdown Spectroscopy (LIBS), SEM-EDS, XRF and LA-ICPMS, NIJ Grantees Meeting AAFS Meeting, Seattle WA (**PA, invited Poster Presentation**)

45. January 2006, Laser Ablation-ICP-MS for the Examination of Trace Evidence, NIJ Applied Technology Conference, Hilton Head, SC (**PA, invited Oral Presentation**)

Appendix C – Copy of each of the publications listed in Appendix A (publications 3-7).